A New Research Proposal submitted to JLab PAC34

Nucleon Resonance Studies with CLAS12 in the Transition from Meson-Baryon to Quark Degrees of Freedom.

T.-S.H. Lee

Argonne National Laboratory, Argonne, IL 60439 USA

H. Avakian, V.D. Burkert, L. Elouadrhiri, V.I. Mokeev*[,†], S. Stepanyan*

Jefferson Lab, Newport News, VA 23606, USA

V.V. Chesnokov, G.V. Fedotov, E.N. Golovach, B.S. Ishkhanov, E.L. Isupov, N.V. Shvedunov

Skobeltsyn Nuclear Physics Institute, Moscow State University, 11989 Moscow, Russia

P. Stoler[*]

Department of Physics, Rensselaer Polytechnic Institute, Troy, NY 12181, USA

K. Joo[*]*, N. Markov, T. Mineeva, M. Ungaro*

University of Connecticut, Storrs, Connecticut 06269, USA

C. Djalali, R.W. Gothe[*,†]*, K. Park, S. Strauch, D. Tedeschi*

Department of Physics and Astronomy, University of South Carolina, Columbia, SC 29208, USA

P.L. Cole[*]*, D.S. Dale, T.A. Forest*

Department of Physics, Idaho State University, Pocatello, ID 83209, USA

I. Aznauryan

Yerevan Physics Institute, 375036 Yerevan, Armenia

A. Biselli

Physics Department, Fairfield University, Fairfield, CT 06824, USA

D. Arndt, W.J. Briscoe, M. Paris I. Strakovsky, R. Workman

Center for Nuclear Studies, Department of Physics, The George Washington University, Washington, D.C. 20052, USA

1

Theory Support Group

B. Julia-Diaz, H. Kamano, A. Matsuyama, T. Sato, N. Suzuki

Excited Baryon Analysis Center at Jefferson Lab, Newport News, VA 23606 USA

C.D. Roberts

Argonne National Laboratory, Argonne, IL 60439 USA

I. Cloet

University of Washington, Seattle WA 98195, USA

R. Edwards, H.W. Lin

Jefferson Lab, Newport News, VA 23606, USA

V.M. Braun, A. Lenz, G. Schierholz

Institut für Theoretische Physik, Universität Regensburg, 93030 Regensburg, Germany

M.V. Polyakov

Institut für Theoretische Physik II, Ruhr Universität, Bochum, D-44780 Bochum, Germany

M.M. Giannini, E. Santopinto

University of Genova and INFN–Genova, Via Dodecaneso 33, Genova, Italy

and the CLAS collaboration

*Spokesperson
†Contact person

1 Participation of Research Groups

1.1 University of South Carolina

The University of South Carolina group is actively involved in this proposal using CLAS12 base equipment. Ralf Gothe is a member of the CLAS12 Steering Committee. Among the CLAS12 baseline equipment, our group has taken responsibility for the design, prototyping, construction and testing of a new forward Time-of-Flight detector panel that will provide the required increased time resolution for particle identification in CLAS12. Ralf Gothe is currently the user representative in the Time-of-Flight technical working group. The USC nuclear physics group is committed to carry out this project and will continue to be fully involved as needed. The group is currently funded by NSF. The University of South Carolina is providing a detector assembly hall for the duration of the project and has funded $ 150,000 for the initial infrastructural needs. Additional sources of funding will be sought as appropriate.

1.2 Moscow State University

The Moscow State University Group (MSU) is actively involved in development of CLAS12 base equipment needed for proposed experiments.

In particular, the MSU group will participate in development of the simulation (GEANT4) and reconstruction software and trigger and data acquisition. The MSU group takes responsibility for the maintenance and development of SVT for CLAS12 Central Detector. MSU will develop and supports the special Data Base needed for N* studies in coupled channel analysis. This Project will be developed jointly with Hall B and EBAC. At least 4 staff scientist and 5 PhD and/or graduate students will be involved in base equipment development. The MSU group takes responsibility for development of physics analysis approaches with a goal of extracting N^* electrocouplings from 2π electroproduction data.

1.3 Rensselaer Polytechnic Institute

The RPI group is actively involved in this proposal using CLAS12 base equipment. Paul Stoler is a member of the CLAS12 Steering Committee. Among the CLAS12 baseline equipment, our group has involved in the design, prototyping, construction and testing of the high threshold and modification of the low threshold Cerenkov detector. Currently, Paul Stoler is serving as a coordinator for the collaboration of groups involved in the effort. Valery Kubarovsky is designing and building the apparatus for testing the prototype components. Two undergraduates Jason Sanchez and Stephanie Tomasulo, are spending the summer at JLab working respectively on prototype mirror fabrication and computer aided optics design and simulation. The group will continue to be fully involved as needed. The group is currently funded by NSF and RPI. Additional sources of funding will be sought as appropriate.

1.4 University of Connecticut

The University of Connecticut (UConn) group is actively involved in this proposal using CLAS12 baseline equipment.

Among the CLAS 12 baseline equipment, our group has taken responsibility for the design, prototyping, construction and testing of the high threshold Cerenkov counter (HTCC). One faculty member, one post-doc, four graduate students are already or will be working at least part time on this project in the next few years. The University of Connecticut Research Foundation (UCRF) already funded $32,000 for the equipment purchase for the HTCC prototyping project. The University is also providing funding for a half postdoctoral support and a half graduate student support for the next two years for the our group's JLab research activities. The group is currently funded by the U.S Department of Energy (DOE). Additional sources of funding will be sought as appropriate.

Beyond the baseline equipment, the group is also deeply involved in software planning and development for CLAS12. The group was recently awarded a DOE SBIR/STTR Phase I grant with a software company, CyberConnect EZ to develop a software framework to archive a large scale nuclear physics experiment data base

1.5 Idaho State University

The Idaho State University group is actively involved in this proposal using CLAS12 base equipment The ISU medium-energy nuclear physics group (Cole, Dale, and Forest) will assemble and string six Region 1 Drift Chambers (R1 DCs) for CLAS12. This large undertaking ($1.5 Million) will have the support of the unique resources and technical staff afforded by the Idaho Accelerator Center (see: http://www.iac.isu.edu/), The Idaho Accelerator Center (IAC) has the most diverse and most numerous collection of research accelerators of any university in the nation. The group has employed two of its 25 MeV electron linacs for characterizing the efficiency of CLAS12 wire chamber prototypes using a single-pulsed electron beam. ISU recently joined SURA as an affiliate member in November, 2008 and marks the first such university to join SURA outside the region besides MIT. ISU has recently hired a JLab-bridged Assistant Professor, Guilio Stancari, whose work will bear upon accelerator physics for the 12-GeV upgrade. The group is funded through the NSF. And will seek additional funding as necessary.

1.6 The George Washington University – Center for Nuclear Studies – Data Analysis Center

The GW Data Analysis Center is actively involved in extensive research program on theoretical interpretation of the results from the proposed experiment. In particular, the GW group will provide an extended analysis of the pi-N, N-N, Gamma-N, and Gamma*-N by the time of 12 GeV Upgrade. The Gamma*-N contribution is essential for the GPD calculations of Ruhr University, Bochum with whom GW is colaborating. Experimentally, we

plan to submit a supplemental proposal to DOE to work with South Carolina (Ralf Gothe) in the development of a needed calibration system for the TOF-12 detector. (Briscoe and Strakovsky)

Theoretical support of Proposal

1.7 Lattice Group at the JLab Theory Center

The Lattice Group at JLAB Theory Center contributors to the Proposal are actively involved in extensive research program on theoretical interpretation of the results from the proposed experiment. In particular, the group will provide LQCD calculations of transition helicity amplitudes and/or related form factors for several excited proton states of various quantum numbers at photon virtualities of the proposed experiment in the time of 12 GeV Upgrade.

1.8 Excited Baryon Analysis Center

The Excited Baryon Analysis Center (EBAC) contributors to the Proposal are actively involved in extensive research program on theoretical interpretation of the results from the proposed experiment. In particular, EBAC will develop analysis method for interpreting extracted N* form factors in $Q^2 = 5 - 10 GeV^2$ in terms of DSE and LQCD predictions in the time of 12 GeV Upgrade.

1.9 Argonne National Lab

The Argonne National Lab (ANL) contributors to the Proposal are actively involved in extensive research program on theoretical interpretation of the results from the proposed experiment. In particular, ANL group will provide a calculations of transition helicity amplitudes and/or related form factors for several excited proton states of various quantum numbers within the framework Dyson-Schwinger approach by the time of 12 GeV Upgrade.

1.10 University of Washington

The University of Washington contributors to the Proposal are actively involved in extensive research program on theoretical interpretation of the results from the proposed experiment. In particular, University of Washington group will provide a calculations of transition helicity amplitudes and/or related form factors for several excited proton states of various quantum numbers within the framework Dyson-Schwinger equations in the time of 12 GeV Upgrade.

1.11   Regensburg University

The Regensburg University contributors to the Proposal are actively involved in extensive research program on theoretical interpretation of the results from the proposed experiment. In particular, University of Washington group will provide a calculations of transition helicity amplitudes and/or related form factors for several excited proton states of various quantum numbers within the framework of a combined Light Cone Sum Rules and LQCD approach in the time of 12 GeV Upgrade.

1.12   University of Genova and INFN of Genova

The University of Genova and INFN of Genova contributors to the Proposal are actively involved in extensive research program on theoretical interpretation of the results from the proposed experiment. In particular, the group will provide fully relativistic calculations of transition helicity amplitudes and/or related form factors for a major part of excited proton states and at photon virtualities covered by the proposed experiment in the time of 12 GeV Upgrade.

2 Introduction

Nucleons and baryons in general, have played an important role in the development of our understanding of the strong interaction. The concept of quarks was first made manifest through the study of baryon spectroscopy, which led to the development of constituent quark models [40, 41] (CQMs) in the 1970s. As a result of intense experimental and theoretical efforts, especially in recent years, it has become clear that the structure of the nucleon and its excited states (N^*) is much more complex than what can be described in terms of constituent quarks. The structure of low-lying baryon states, as revealed by electromagnetic probes at low momentum transfer, can be understood reasonably well by adding meson-baryon effects phenomenologically to the predictions from constituent quark models [42–46]. However, a fundamental understanding of the properties of the nucleon and its excited states at short distances, which are accessible using probes with sufficiently high momentum transfer, demands the full machinery of Quantum Chromodynamics (QCD). In recent years, there has been tremendous progress in this direction. Constituent quark models have been greatly refined by using fully relativistic treatments [43, 44, 46] and by including sea quark components [47]. Hypercentric CQM with improved treatment of constituent quark interactions [45] emerges. A covariant model based on the Dyson-Schwinger equations [48] (DSE) of QCD is now emerging as a well-tested and well-constrained tool to interpret baryon data directly in terms of current quarks and gluons. This approach also provides a link between the phenomenology of dressed current quarks and Lattice QCD (LQCD). Relations between baryon form factors and the Generalized Parton Distributions (GPDs) have also been formulated [49, 50] that connect these two different approaches for describing baryon structure. On a fundamental level, Lattice QCD is progressing rapidly in making contact with the baryon data. The USQCD Collaboration, involving JLab's LQCD group, has been formed to perform calculations for predicting the baryon spectrum and N-N^* transition form factors.

On the experimental side, extensive data on electromagnetic meson production have been obtained at JLab, MIT-Bates, LEGS, MAMI, ELSA, and GRAAL in the past decade. The analyses of these data and the data expected in the next few years before the start of experiments with the JLab 12-GeV upgrade, will resolve some long-standing problems in baryon spectroscopy and will provide new information on the structure of N^* states. To enhance this effort, the Excited Baryon Analysis Center (EBAC) was established in 2006 and is now making rapid progress in this direction. In addition to extracting N^* parameters from the data, an important aim of EBAC is to develop rigorous approaches to interpret the extracted N^* information in terms of what can be predicted by CQMs, DSE, and LQCD. Significant progress from this experiment-theory joint effort has been made in the past few years. Here we give several examples.

To confront the challenge presented by the precise data on N-$\Delta(1232)$ transition form factors, quenched and full LQCD calculations [51] have been performed and are being improved. In the left side of Fig. 1, we show the LQCD results that reproduce the main features of the empirical values extracted by EBAC using a dynamical approach [52]. On the right side of Fig. 1, the most recent LQCD calculations [53] of the $F_{1,2}(Q^2)$ form factors
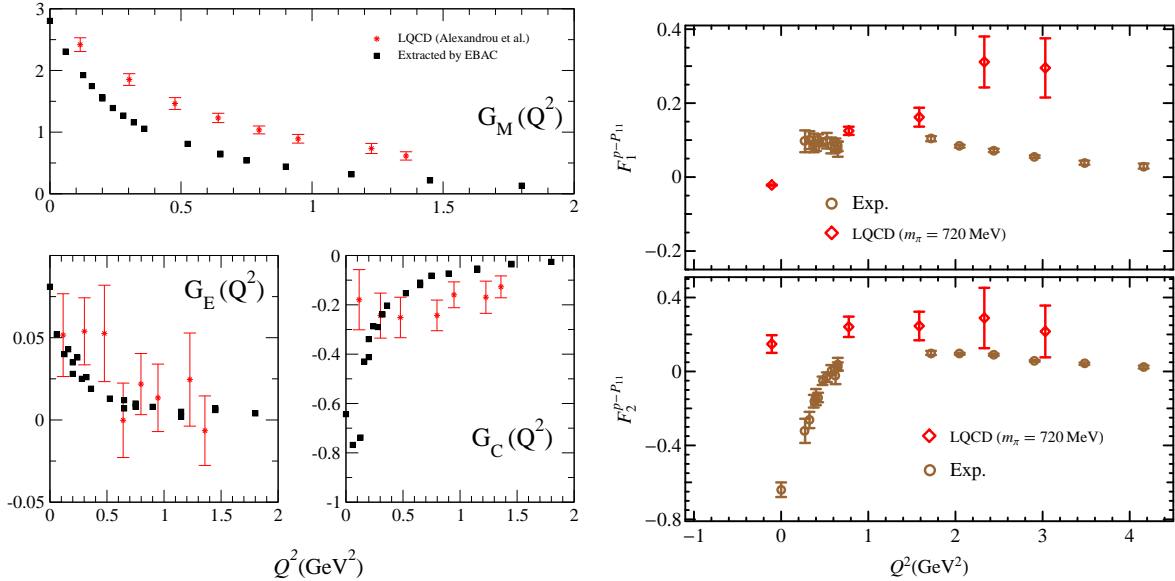
Figure 1: Lattice QCD calculations of transition form factors. Left panel: N-$\Delta(1232)$ transition form factors G_M, G_E, and G_C vs Q^2. Empirical values (solid squares) are extracted by EBAC from world data within a dynamical model. The LQCD results are from Ref. [51]. Right panel: $F_1(Q^2)$ and $F_2(Q^2)$ for the N-$P_{11}(1440)$ transition. Empirical values are from the CLAS Collaboration [109, 172] and the LQCD results are from Ref. [53].

of the N-$N^*(1440)$ transition are compared with the precise data extracted by the CLAS Collaboration and other groups. While these LQCD results extracted from calculations with large pion masses are still very preliminary, rapid progress is expected from the efforts of the USQCD Collaboration.

Another approach based on LQCD calculations was recently proposed in order to relate N^* electrocoupling parameters to QCD [54, 55]. In this approach, LQCD is used to obtain several moments of the resonance Distribution Amplitudes (DAs). The N^* electrocoupling parameters are then determined from the DAs within the framework of Light Cone Sum Rules (LCSR) methods [56]. This technique is applicable at photon virtualities $Q^2 > 2.0$ GeV^2. Therefore, data from the proposed experiment are needed in order to utilize this approach for resonance structure analyses. Fig. 2 shows the N-$N^*(1535)$ transition amplitudes. These calculations will be extended to other resonances as part of the commitment by contributors from the Institut für Theoretische Physik, the Universität Regensburg, and DESY in theoretical support of our proposal.

A third example of recent progress in N^* physics is given in Fig. 3. It shows that high precision N-N^* transition form factors and helicity amplitudes are becoming available from the world-wide effort in analyzing the data from JLab and other facilities. Furthermore, the CQM has been greatly refined to confront these data by implementing fully relativistic treatments [43–46] or incorporating sea quark contributions [47]. In Fig. 3, the results of a recent relativistic CQM calculations are compared with the extracted experimental results
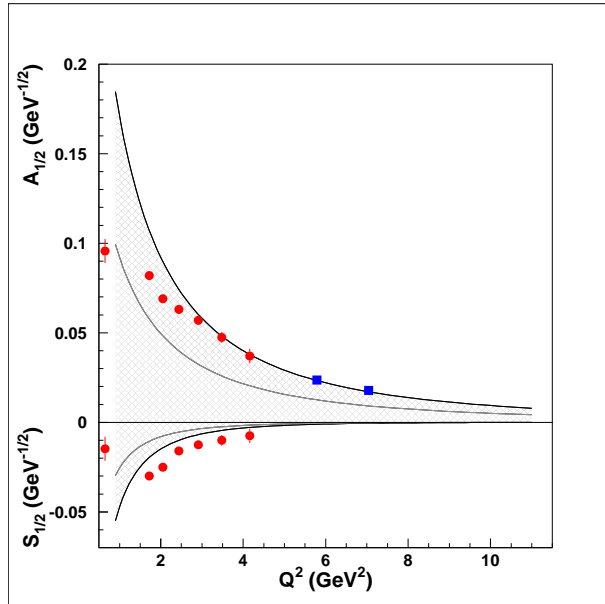
Figure 2: Transition N-$N^*(1535)$ amplitudes based on LCSR, that utilized preliminary LQCD results of Distribution Amplitudes [55] in comparison with the data. CLAS data [109]are shown in red, while preliminary data on $(A_{1/2}^2 + \epsilon S_{1/2}^2)^{1/2}$ combination of transition amplitudes at high Q^2 are shown in blue.

for the transitions N-$\Delta(1232)$, N-$N^*(1440)$, and N-$N^*(1520)$. We see that they are in reasonably good agreement with the data at high Q^2, but deviate from the empirical values significantly at low Q^2. In the same figure, we also show the contributions from meson-baryon dressing of resonance electromagnetic vertices to transition amplitudes and resonance form factors predicted by the dynamical model [52, 57–59] developed at EBAC. For the N-$\Delta(1232)$ case, it has been shown [52, 60, 61] that the data can be reproduced reasonably well by including the meson-baryon dressing contributions to the predictions of the CQM. For the N-$N^*(1440)$ and N-$N^*(1520)$ transitions, it remains to be seen whether this will be the case in a complete coupled-channels analysis of the world data on $\pi N, \gamma^* N \to \pi N, \pi\pi N, \eta N, KY, \omega N$ reactions that is currently being performed at EBAC. However, the results in Fig. 3 clearly demonstrate substantial meson-baryon contributions at photon virtualities covered by the 6.0 GeV N^* program with CLAS.

The results from the analysis of the already available data and those that will be obtained in the next few years at JLab, will provide the foundation of N^* information up to $Q^2 \simeq$ 5 GeV^2. At these distance scales the resonance structure is determined by both meson baryon dressing and dressed quark contributions. Here we propose to perform experiments that extend this information into the $Q^2 > 5.0$ GeV^2 regime, and to determine the Q^2-evolution of the corresponding electrocoupling parameters for N^* states with masses less than 2 GeV using exclusive channels: $ep \to ep\pi^0$, $ep \to ep\eta$, $ep \to en\pi^+$, and $ep \to ep\pi^+\pi^-$. All channels will be measured simultaneously with the CLAS12 detector, and an extensive
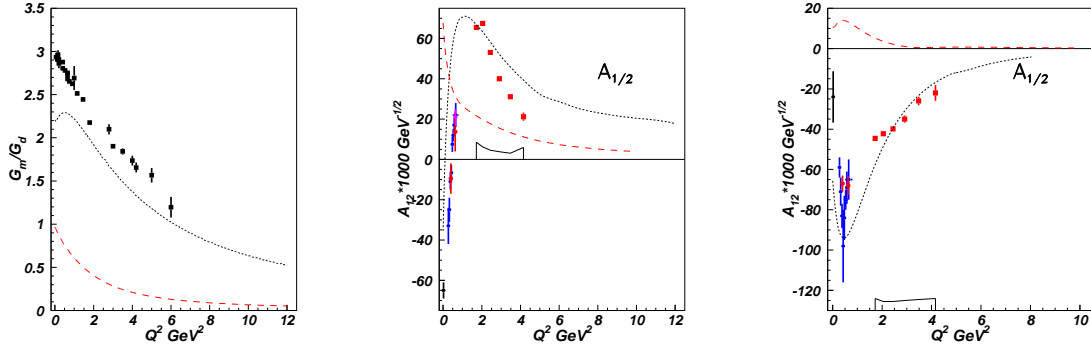
Figure 3: The N-N^* transition form factors and helicity amplitudes. Left panel: Magnetic form factor for the N-$\Delta(1232)$ transition normalized to the dipole form factor. Center panel: Transition helicity amplitude $A_{1/2}$ for N-$N^*(1440)$. Right panel: Transition helicity amplitude $A_{1/2}$ for N-$N^*(1520)$. The results from CLAS/world experimental data analyses are shown by the data points [109, 149–151, 172]. The red and blue symbols are the results from analyses of 1π and 2π exclusive channels, respectively. The curves are from CQM calculations (dotted) and from meson-baryon dressing contributions predicted by EBAC (dashed).

database for N^* studies will be created from the proposed measurements.

The first objective is to map out the quark structure of N^*s from the data of exclusive meson electroproduction reactions. This is motivated by the results shown in Fig. 3, where we see that the meson-baryon dressing contribution decreases rapidly with Q^2 and that the data can be approximately described in terms of dressed quarks. Thus the data at $Q^2 > 5$ GeV^2 can be used more directly to probe the quark substructure of N^*s. Here we note that the meson-baryon dressing shown in Fig. 3 are calculated [59] with parameters that are heavily constrained by fitting a very extensive data set of $\pi N \to \pi N, \pi\pi N$ reactions up to an invariant mass of $W = 2$ GeV and $\gamma N \to \pi N$ reactions up to $W = 1.6$ GeV, which makes the phenomenologically predicted Q^2-dependence realistic. The comparison of the resonance electrocoupling parameters at $Q^2 > 5.0$ GeV^2 to the LQCD results that are expected by the time of the 12-GeV upgrade [54] will allow us to better understand how the internal core of dressed quarks emerges from QCD and how the strong interaction is responsible for the formation of N^* states.

The second objective is to investigate the dynamics of dressed quark interactions inside the nucleon core and to understand how these interactions emerge from QCD. We are motivated by the recent advance in developing hadron models based on the Dyson-Schwinger equations of QCD [67–69]. This approach has provided the links between the dressed quark propagator, dressed quark scattering amplitudes, and the QCD Lagrangian. The electromagnetic form factors of the ground and excited proton states can thus be determined by applying the Bethe-Salpeter/Faddeev equations [70, 71] to a bound system of three dressed quarks with properties and binding interactions that are derived from QCD. In this way

10

the experimental information on the baryon electrocoupling parameters can be related to the interaction of dressed quarks and eventually to QCD. DSE analyses of N^* electrocoupling parameters have the potential to open up new opportunities to investigate the origin of dressed light quark confinement in baryons and the nature of dynamical chiral symmetry breaking, since both of these phenomena, which dominate the physics of hadrons, are rigorously incorporated into DSE approaches. The first studies of nucleon form factors within the framework of DSE have just been completed [72]. The calculated ratio $\mu_p G_E/G_M$ of the elastic proton form factors, shown in Fig. 4, agrees well with the experimental data at $Q^2 > 3.0$ GeV^2, where the quark core starts to dominate. The discrepancy at low Q^2 is due to the neglect of meson-baryon dressing effect in this DSE calculation. Work is being done to resolve this problem discrepency.
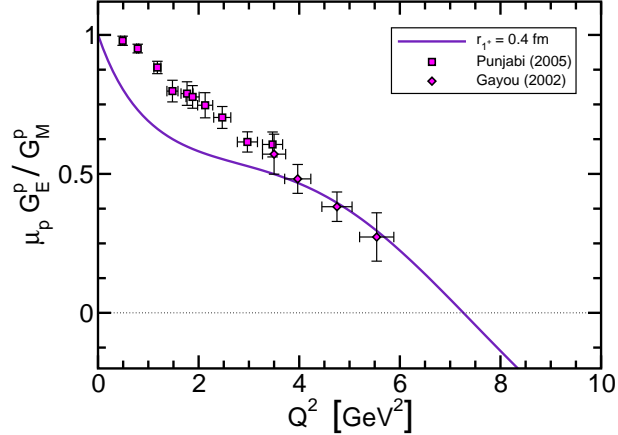

Figure 4: Ratio $\mu_p G_E^p/G_M^p(Q^2)$ of the proton form factor. The solid curve is calculated from the covariant model based on the Dyson-Schwinger equation [72].

The DSE extension for the evaluation of the N-N^* transition amplitudes is in progress [54], and by the time experiments with the 12-GeV upgrade will take data, we expect to have DSE calculations of transition form factors to several excited proton states. This is a part of the commitment of the University of Washington and Argonne National Lab in support of this proposal.

The third objective is to study the Q^2-dependence of non-perturbative dynamics of QCD. This is based on the recent investigation of the momentum (p)-dependence of the dressed quark mass function $M(p)$ of the quark propagator within LQCD [73] and DSE [67]. These results are shown in Fig. 5. We see that $M(p)$ approaches a current quark mass of a few MeV only in the high-momentum region of perturbative QCD. As the momentum p decreases, the current quark is dressed by gluons and acquires a constituent mass of about 300 MeV, a value that is typically used as a fixed parameter in constituent quark models. This result predicted by DSE was confirmed by LQCD. Experimental verification of this momentum dependence would further advance our understanding of non-perturbative QCD dynamics. Efforts are currently underway [54] to study the sensitivity of the proposed transition form

factor measurements to different parameterizations of the momentum dependence of the quark mass. We emphasize here that we are not aiming at examining the transition to perturbative QCD in the Q^2 regime considered. Instead, our focus is on the important question about how baryon structure emerges from confinement and the dynamical chiral symmetry breaking of QCD.
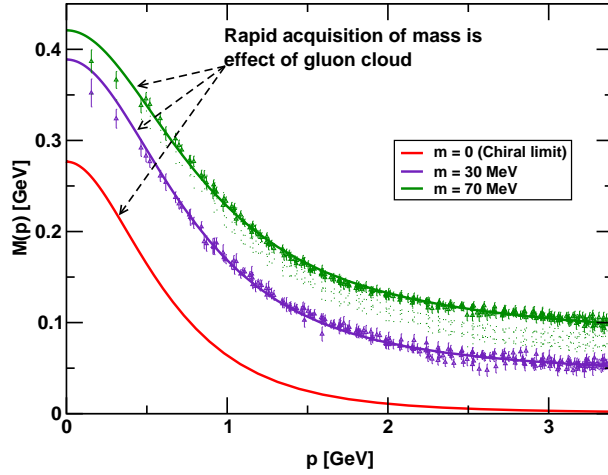

Figure 5: Running quark masses. The solid circles with errors bars are from LQCD calculations with different lattice spacing characterized by the pion mass M. The curves are from DSE.

Here we also note that the results of running quark masses shown in Fig. 5 suggest that the CQM now has some justifications from QCD. Thus the agreements between the CQM calculations and the extracted N-N^* form factors at high Q^2 seen in Fig. 3 suggest that CQM can be used in initial phenomenological analyses of resonance electrocoupling amplitudes from the proposed experiments. Compared with DSE, their merit is simplicity. While the systematic connection between CQM and QCD has not been rigorously established, the current relativistic CQM [43, 44, 46] are the only available analysis tool for studies of the electrocoupling amplitudes of the majority of N^* states. Fully relativistic treatment will be incorporated also in the model [45] by the time of 12 GeV Upgrade. Exploiting CQM will allow us to pin down the active degrees of freedom, such as either 3-quark or quark-diquark configurations and the sea quarks in resonances [47], as well as the quark interactions at various distance scales [74]. This is an important phenomenological piece of information for the understanding how fundamental QCD interactions between pointlike quarks and gauge gluons evolve to effective interactions and degrees of freedom utilized by CQM. These studies will also allow us to constraint N^* light cone wave functions (LCWF). Several approaches are being developed with the goal of relating LCWF to QCD [75].

Finally, we point out that the proposed experiments are closely related to the GPD program of JLab. The characterization of exclusive reactions at high momentum transfer in terms of GPDs is a major goal of the CLAS12 upgrade. Experiments already approved as part of this program include deeply virtual Compton scattering (DVCS) and deeply virtual meson

production (DVCS). The elastic and N-N^* transition form factors are the first moments of the GPDs, and they uniquely provide important constraints on fully unexplored N-N^* transition GPDs. Therefore, information on N-N^* transition form factors from our proposed experiment will offer a vital contribution to the overall exclusive reaction program.

Figure 6 shows a fit to the $N \rightarrow \Delta$ form factor G_M^*, which is obtained by GPDs constrained from elastic scattering, and the extracted transverse impact parameter distribution vs. fraction of longitudinal momentum fraction x. The transition form factors of all of the resonance in this proposal can be directly connected to their respective GPDs, and through them provide the constraints on the theoretically calculated overlap integrals. The relationships of baryon transition form factors to GPDs is treated in the next section.
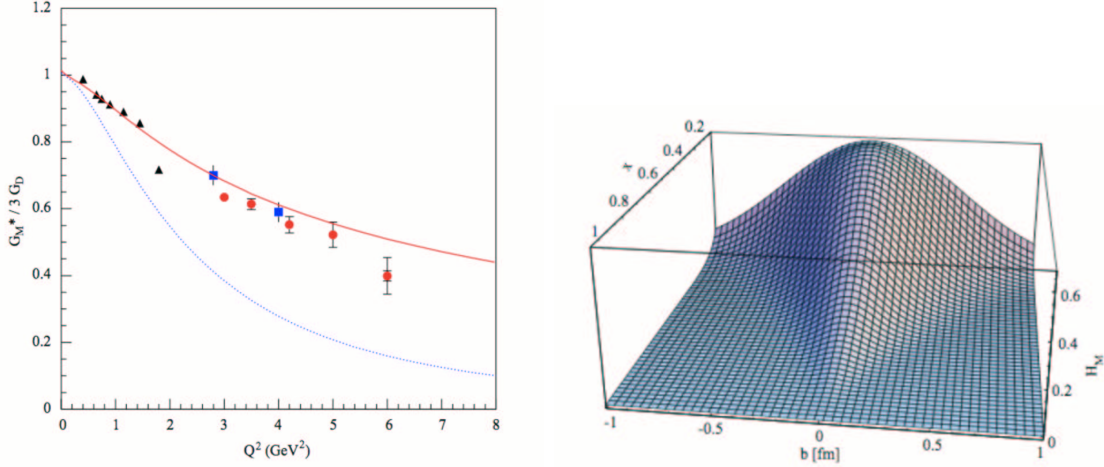

Figure 6: (Left) The red curve represents the form factor G_M^* obtained by using a Regge like parameterization of the elastic isovector form factor applied to the $N \rightarrow \Delta$ transition. (Right) The distribution of the transverse impact parameter $\vec{b}_\perp$ and longitudinal momentum [49].

The experiment proposed here provides the needed experimental data on the Q^2 evolution of the transition form factors in a still unexplored domain of photon virtualities above 5 GeV^2. For the foreseeable future, CLAS12 is the only facility that will be capable of investigating the structure of excited nucleon states at distance scales where quark degrees of freedom are expected to dominate. The extraction of the N-N^* transition amplitudes for the majority of excited proton states from the comprehensive data based on this experiment together with information provided by the already approved experiments of the 12 GeV Upgrade Research Program will open up a challenging opportunity to understand how the strong interaction of dressed quarks creates excited nucleon states and how these interactions emerge from QCD. Our proposed experimental and theoretical effort offers a unique opportunity to probe the mechanisms responsible for the formation of more than 97% of the hadronic mass in the Universe, that is expected to originate from the dynamical dressing of light current-quarks by gluons.

2.1 Connection of Baryon Form Factors and GPDs

Nucleon elastic and transition form factors are the first moments of the GPDs. Their relationship to the GPD program is illustrated in Fig. 7. The relationships between GPDs and resonance form factors were worked out several years ago [12, 13]. Here we consider their application to transitions involving several of the resonances which are central to this proposal, ie. the $\Delta(1232)$, $P_{11}(1440)$ and $S_{11}(1535)$.

Figure 7: Various reactions which can contribute to the characterization of GPDs

The $N \to \Delta(1232)$:

The first practical application of GPDs to resonances were reported in [14] for the $N \to \Delta(1232)$ transition. The current structure of the transition $\Gamma_{\nu\mu} = G_M^*(q^2)K_{\nu\mu}^M(q^2) + G_E^*(q^2)K_{\nu\mu}^E(q^2) + G_C^*(q^2)K_{\nu\mu}^C(q^2)$ leads to the following GPD relation:

$$\frac{1}{2\pi} \int dy^- e^{ix\bar{P}^+ y^-} \langle \Delta(p')| \, \bar{\psi}\left(-y/2\right) \gamma_\mu n^\mu \tau_3 \psi\left(y/2\right) |N(p)\rangle \Big|_{y^+ = \vec{y}_\perp = 0} =$$

$$\bar{u}_\Delta(p') \left\{ H_M(q^2)K_{\nu\mu}^M(q^2) + H_E(q^2)K_{\nu\mu}^E(q^2) + H_C(q^2)K_{\nu\mu}^C(q^2) \right\} n^\mu u_p(p)$$

with

$$2G_M^*(t) = \int dx\, H_M(t, x, \xi), \quad 2G_E^*(t) = \int dx\, H_E(t, x, \xi) \quad \text{and} \quad 2G_C^*(t) = \int dx\, H_C(t, x, \xi)$$

Thw $N \to \Delta$ transition, is purely purely isovector and in certain approximations H_M can be directly related to the isovector part of the elastic GPD $E_{elastic}$, which is mostly isovector. Thus, it was possible to demonstrate that the anomalous falloff G_M^* with Q^2 is directly related to the anomalous falloff of the elastic Pauli form factor F_2. Figure 6 shows the result of a more recent analysis by ref. [**?**], in which the the form of the elastic GPD for the nucleon was parameterized by a Regge-like prescription, and the isovector part applied to obtain the Δ H_M GPD. Figure 6 shows H_M vs. x, and $\vec{b}_\perp$. This is an example of how the GPD of one resonance can reveal the structural relationships of the partonic distribution amplitudes of the ground state with the excited states. These relationships must also map onto the calculations of the GPDs for elastic scattering and transitions from the nucleon's ground state to its excited states. The Fourier transform of the GPD gives the distribution of the impact parameter [**?**] in the transverse plane vs. the longitudinal momentum fraction, 1.e. $H_M(\vec{b}_\perp, x)$:

$$H_M(x, \vec{b}_\perp) = \int \frac{d^2(\vec{q}_\perp)}{2\pi^2} e^{i(\vec{b}_\perp \cdot \vec{q}_\perp)} H_M(-\vec{q}_\perp^2, x, 0).$$

The relationship of the GPD formalism and nucleon excitation is most readily seen in the $J = 1/2 \to 1/2$ transitions such as the $N \to P_{11}(1440)$ or the $S_{11}(1535)$.

The N → P$_{11}$(1440): Since the $N \to P_{11}(1440)$ is a $1/2^+ \to 1/2^+$ transition, its current structure is similar to elastic scattering, i.e.

$$\Gamma_\mu^{P11} = \frac{F_1^{P11}(q^2)}{M_N^2}\left(q^2\gamma_\mu - \slashed{q}q_\mu\right) + \frac{F_2^{P11}(q^2)}{2M_N}i\sigma_{\mu\nu}q_\nu$$

which immediately leads to a GPD structure and related form factors exactly as in elastic scattering:

$$\frac{1}{2\pi}\int dy^- e^{ix\bar{P}^+y^-}\left.\langle P_{11}(p')|\,\bar{\psi}\left(-y/2\right)\gamma n\psi\left(y/2\right)|N(p)\rangle\right|_{y^+=\vec{y}_\perp=0} =$$

$$H^{P11}\bar{u}(p')\frac{(q^2\gamma_\mu - \slashed{q}q_\mu)}{M_N^2}u(p) + E^{P11}\bar{u}(p')i\sigma^{\mu\nu}\frac{n_\mu q_\nu}{2M_N}u(p)$$

$$F_{1P_{11}}^q(t) = \int H_{P_{11}}^q(x,\xi,t)dx \quad F_{2P_{11}}^q(t) = \int E_{P_{11}}^q(x,\xi,t)dx$$

The N → S$_{11}$(1535): The $S_{11}(1535)$ has $J^\pi = 1/2^-$ and is the chiral negative parity partner of the nucleon. The current structure has an extra γ_5 and is

$$\Gamma_\mu^{S11} = \frac{F_1^{S11}(q^2)}{M_N^2}\left(q^2\gamma_\mu - \slashed{q}q_\mu\right)\gamma_5 + \frac{F_2^{S11}(q^2)}{2M_N}i\sigma_{\mu\nu}q_\nu\gamma_5$$

which leads to

$$\frac{1}{2\pi}\int dy^- e^{ix\bar{P}^+y^-}\left.\langle S_{11}(p')|\,\bar{\psi}\left(-y/2\right)\gamma n\psi\left(y/2\right)|N(p)\rangle\right|_{y^+=\vec{y}_\perp=0} =$$

$$H^{S11}\bar{u}(p')\frac{(q^2\gamma_\mu - \slashed{q}q_\mu)}{M_N^2}\gamma_5 u(p) + E^{S11}\bar{u}(p')i\sigma^{\mu\nu}\gamma_5\frac{n_\mu q_\nu}{2M_N}u(p)$$

with

$$F_{1S_{11}}^q(t) = \int H_{S_{11}}^q(x,\xi,t)dx \quad F_{2S_{11}}^q(t) = \int E_{S_{11}}^q(x,\xi,t)dx$$

Similar expressions for other large resonances with higher spin, such as $D_{13}(1520)$ and $F_{15}(1680)$, involve more Dirac structure elements than spin 1/2 states, but can equally be constructed.

2.2 Expected data base and analysis approaches

This proposal is aims to measure the evolution of the transition form factors to the excited nucleon quantum states over a range of Q^2 from 4.0 to 14 GeV^2. We expect that there will be a contemporaneous evolution in the theoretical tools for describing the evolution from the long range to the short range structure of these nucleon quantum states.

We propose to determine Q^2-evolution of electrocouplings for N^* states with masses less than 3 GeV, including possible new baryon states, from the analysis of two major exclusive channels: $ep \rightarrow ep\pi^0$, $ep \rightarrow en\pi^+$, and $ep \rightarrow ep\pi^+\pi^-$ ($ep \rightarrow ep\eta$ will be measured as well). All channels will be measured simultaneously with *CLAS12*. An extensive data base for N^* studies will be created from the proposed measurements.

For the $\pi^+ n$ and $\pi^0 p$ channels the following observables will be measured in each W and Q^2 bin:

- complete azimuthal and polar angular distributions for π^+, π^0

- polarized beam asymmetries A_e

Data on $\pi^-\pi^+ p$ production for each W and Q^2 bin will consist of:

- $\pi^-\pi^+$, $\pi^+ p$, $\pi^- p$ invariant mass distributions

- π^+, π^-, p cm-angular distributions

- 3 distributions over angles between two planes, composed by two pairs of 3-momenta of the final hadron for 3 various choices of hadron pairs

Overall 18 observables in each bin will be available to evaluate the N^* electrocouplings in a combined analysis of single and double pion production.

In the first stage, the N^* electrocouplings will be extracted in fits to the 1π and 2π channels combined, but neglecting their mutual couplings. Phenomenological approaches have been developed for that purpose [? ?]. These two approaches will be applied separately for the two channels, however all data will be fitted with a common set of N^* electrocouplings. Successful fit of all observables in two major exclusive channels will provide initial information on N^* electrocouplings. A final evaluation of N^* electrocouplings will be carried out within the framework of the most advanced coupled channel approach, which is now under development within the Excited Baryon Analysis Center (EBAC) at the JLab Theory Center. This approach is discussed in detail in Sect. 4.2-4.5. From such a procedure we expect reliable results on N^* electrocouplings. Moreover, the result of this analysis will have strong impact on N^* studies in all other exclusive channels. Single and double pion production, being major contributors, should affect considerably all other exclusive reactions through channel couplings.

The next three sections describe in more detail the basic motivation for for studying the properties of baryon resonances over a large range of Q^2. Section 2 deals with single meson electroproduction, which historically has been the subject of most in-depth work. Section 3 then discusses two meson electroproduction, and its potential for augmenting single meson production as an equal partner in the expanded experimental program. Section 4 then explores the most vital question of what we will do with this plethera of data forthcoming from the experimental program. That is, how we will put it all together in a coupled channel approach to extract the photo-couplings for the individual N* resonances.

3 N^* studies in meson electroproduction with CLAS

The comprehensive experimental data set obtained with the CLAS detector on single pseu-doscalar meson electroproduction, e.g. $p\pi^0$, $n\pi^+$, $p\eta$, and $K\Lambda$ [76–90] and double charged pion electroproduction [145, 147, 148] opens up new opportunities for studies of the N-N^* transition helicity amplitudes (i.e. the N^* electrocoupling parameters) [149–151]. The CLAS data for the first time provides information on a large amount of observables in these exclu-sive channels, including fully integrated cross sections and a variety of 1-fold differential cross sections complemented by single and double polarization asymmetries in a wide area of pho-ton virtualities from 0.2 to 4.5 $(\mathrm{GeV}/\mathrm{c})^2$. This comprehensive information makes it possible to utilize well established constraints from dispersion relations and to develop phenomeno-logical approaches for the Q^2 evaluation of the N^* electrocoupling parameters by fitting them to all available observables in a combined approach. Several phenomenological analyses of the experimental data that have already been carried out within the CLAS Collaboration [105, 108, 109, 171–173] have allowed us to determine transition helicity amplitudes and or the correspond transition form factors for a variety of low lying states: $P_{33}(1232)$, $P_{11}(1440)$, $D_{13}(1520)$, $S_{11}(1535)$ at photon virtualities from 0.2 to 4.5 $(\mathrm{GeV}/\mathrm{c})^2$. Typical examples for resonance electrocoupling parameters are shown in Figures 14, 15, and 17. The analysis of our 2π data allowed us for the first time to map out the Q^2 evolution of electrocoupling parameters for resonances with masses above 1.6 $\mathrm{GeV}/\mathrm{c}^2$ that preferably decay by 2π emis-sion: $S_{31}(1620)$, $D_{33}(1700)$ and $P_{13}(1720)$ [169]. In this analysis we observed a signal from a $3/2^+(1720)$ candidate state whose quantum numbers and hadronic decays parameters are determined from the fit to the measured data [145].

Nucleon resonances contribute to the electroproduction of mesons in the s-channel pro-cesses shown in Figure 8. There are up to three transition helicity amplitudes $A_{1/2}(Q^2)$, $A_{3/2}(Q^2)$, and $S_{1/2}(Q^2)$, that fully describe excitation of a resonance by virtual photons. Resonance excitations may be also described in terms of $F_1^*(Q^2)$, $F_2^*(Q^2)$ or $G_E^*(Q^2)$, $G_M^*(Q^2)$ transition form factors (for states with spin$> 1/2$ we also have third form factor in both rep-resentations), that are very often used in the electromagnetic $N \to N^*$ transition current. They play a similar role as the elastic form factors. The descriptions of resonance excita-tions by transition form factors or transition helicity amplitudes are equivalent and can be uniquely expressed by each other [88]. They can be determined either by fitting resonances within the framework of a Breit-Wigner ansatz [156] or by applying various multi-channel resonance parameterizations [152].

In order to determine the N^* helicity amplitudes a reliable separation of resonant and non-resonant parts contributing to the meson electroproduction amplitudes is needed. This is one of the most challenging problems for the extraction of N-N^* electrocoupling parameters. The amplitudes of effective meson-baryon interactions in exclusive electroproduction reactions cannot be expanded over a small parameter over the entire resonance region. It is impossible to select contributing diagrams through a perturbative expansion. So far, no approach has been developed that is based on a fundamental theory and that would allow either a description of an effective meson-baryon Lagrangian or a selection of the contributing
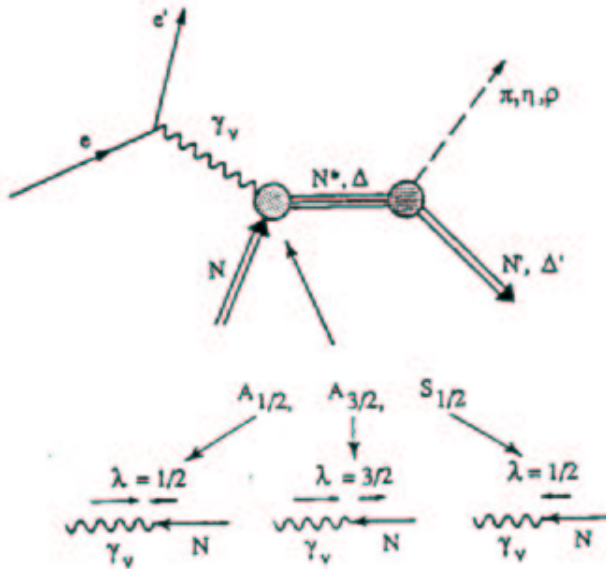
Figure 8: Resonant amplitudes in meson electroproduction. Six amplitudes, corresponding to various helicities of the initial photon-proton state, fully describe the N^* electroexcitation. Parity conservation reduces the number of independent amplitudes to three: two transverse $A_{1/2}$ (non-spin-flip) and $A_{3/2}$ (spin flip), and one longitudinal $S_{1/2}$.. Corresponding transition form factors are then given by unique linear combinations of these helicity amplitudes.

meson-baryon mechanisms from first principles. We therefore have to rely on fits to the comprehensive experimental data of various meson electroproduction channels from CLAS to develop reaction models that contain the relevant mechanisms. Therefore the isolation of the resonant contributions can only be carried out at phenomenological level. This approach allows us to determine all the essential contributing mechanisms in terms of relevant meson-baryon isobar channels and hadronic final states that are created without the formation of unstable hadrons in the intermediate states, the so-called direct production mechanisms.

As illustrated in Figure 8, nucleon resonances have various decay modes and hence manifest themselves in different meson electroproduction channels. Contributions of non-resonant amplitudes are substantially different in the different meson electroproduction channels [97, 151]. On the other hand, the N^* electrocoupling parameters are independent of the specific meson electroproduction channel. They are fully determined by the photon-proton-N^* vertices and independent from the hadronic decay of the resonance. The successful description of a large body of observables in various exclusive channels with a common set of N^* electrocoupling parameters offer compelling evidence for the reliable evaluation of N-N^* helicity amplitudes. Eventually this analysis will be carried out in a complete coupled channel approach which is currently developed at EBAC [99–101].

As shown in Figure 9, single (1π) and double charged (2π) pion electroproduction are the two dominating exclusive channels in the resonance region. The 1π exclusive channel is mostly sensitive to N^*'s with masses lower than 1.65 GeV/c^2. Many resonance of heavier
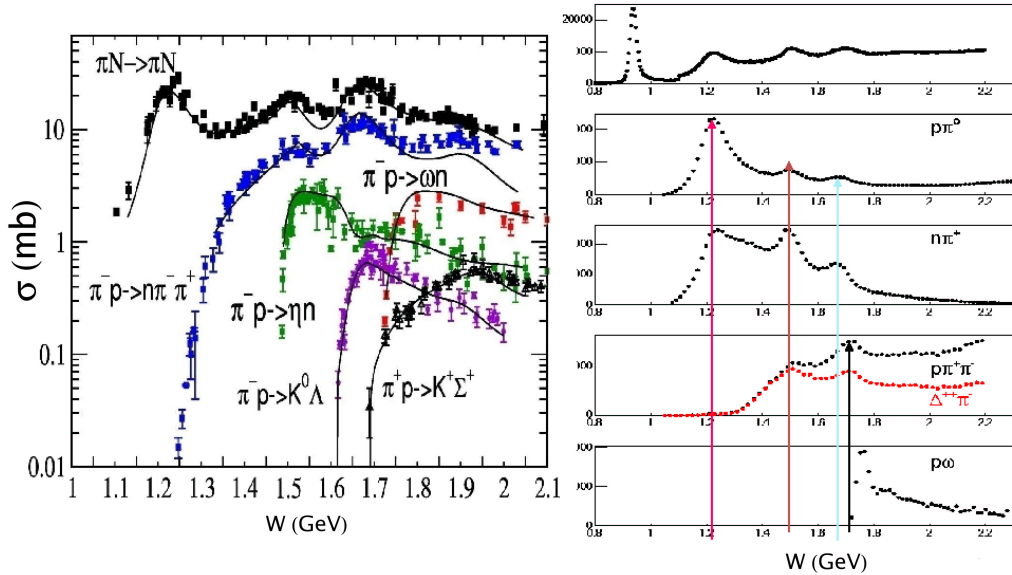
Figure 9: The right panel shows CLAS meson electroproduction yields in various exclusive final state channels at photon virtualities $Q^2 < 4.0$ $(\text{GeV}/c)^2$, and the left panel shows cross section data of the dominant exclusive reaction channels in πN scattering [97].

masses preferably decay by two pion emission. Thus the 2π exclusive channel offers better opportunities to study the electrocoupling parameters of these high-lying states. The final states in 1π and 2π channels have considerable hadronic interactions, as demonstrated in Figure 9 (left panel), where the cross section for the $\pi N \to \pi\pi N$ reaction is the second largest of all of the exclusive channels for πN interactions. Therefore, for N^* studies both in single and double pion electroproduction, information on the mechanisms contributing to each of these channels is needed in order to take properly into account the impact from coupled-channel effects on the exclusive channel cross sections. The knowledge of single and double pion electroproduction mechanisms becomes even more important for N^* studies in channels with smaller cross sections such as $p\eta$ or $K\Lambda$ and $K\Sigma$ production, as they can be significantly affected in leading order by coupled-channel effects produced by their hadronic interactions with the dominant single and double pion electroproduction channels. Comprehensive studies of the single and double pion electroproduction, as proposed here, are of key importance for the entire baryon resonance research program.

19

4   Analysis approaches for the single meson electroproduction data

Over the past 40 years, our knowledge of electromagnetic excitations of nucleon resonances was mainly based on the single-pion photo- and electroproduction. These reactions have been the subject of extensive theoretical studies based on dispersion relations and isobar models. The dispersion relation (DR) approach has been developed on the basis of the classical works [102, 103] and played an extremely important role in the extraction of the resonance contributions from experimental data. The importance of using of this approach is connected to its strict constraints on the real part of the reaction amplitudes that contain the most significant part of the non-resonant contributions. Starting in the late 90s, another approach, the Unitary Isobar Model [104] (also known as MAID), became widely used for the description of single-pion photo- and electroproduction data. Later this approach has been modified [105] by the incorporation of Regge poles. This extension of the isobar model enables a good description of all photo-production multipole amplitudes with angular momenta $l \leq 3$ up to an invariant mass $W = 2\,GeV$ using a unified Breit-Wigner parametrization of the resonance contributions in the form as proposed by Walker [106]. Dispersion relations and this Unitary Isobar Model (UIM) [105] have been successfully used for the analysis [107–109] of the CLAS [110–115] and the world data to extract cross sections and longitudinally polarized electron beam asymmetries for the reactions $p(\vec{e}, e'p)\pi^0$ and $p(\vec{e}, e'n)\pi^+$ in the first and second resonance region. The quality of these results is best characterized by the following χ^2 values: $\chi^2 < 1.6$ at $Q^2 = 0.4$ and $0.65\,(GeV/c)^2$ and $\chi^2 < 2.1$ at $1.72 < Q^2 < 4.16\,(GeV/c)^2$. In the analyses [107–109], the Q^2 evolution of the electrocoupling amplitudes for the lower-lying resonances with $W < 1.6\,GeV$ have been established for Q^2s up to $4.5\,(GeV/c)^2$. The comparison of two conceptually different approaches, DR and UIM, allows to draw the conclusion that the model dependence of the obtained results is relatively small.

The background in both approaches, DR and UIM, contains Born terms corresponding to s- and u-channel nucleon exchanges and the t-channel pion contribution, and thus depends on the proton, neutron, and pion form factors. The background of the UIM contains also the ρ and ω t-channel exchanges, and thus contributions of the form factors $G_{\rho(\omega)\to\pi\gamma}(Q^2)$. The proton magnetic and electric form factors as well as the neutron magnetic form factor are known from the existing experimental data, for Q^2s up to 32, 6, and 10 $(GeV/c)^2$, respectively [116–126]. This information on the proton and neutron elastic form factors combined with the parametrization of the proton electric form factor from polarization experiments [127] can be readily used for the analysis of the pion electroproduction data up to quite large values of Q^2. The neutron electric form factor, $G_{E_n}(Q^2)$, is measured up to $Q^2 = 1.45\,(GeV/c)^2$ [128]. and Ref. A parametrization of all existing data on $G_{E_n}(Q^2)$ [128] can be used to extrapolate $G_{E_n}(Q^2)$ to higher four momentum transfers. The pion form factor $G_\pi(Q^2)$ has been studied for Q^2 values from 0.4 to $9.8\,(GeV/c)^2$ at CEA/Cornell [129, 130] and more recently at JLab [131, 132]. All these measurements show that the Q^2 dependence

of $G_\pi(Q^2)$ can be described by a simple monopole form $1/(1 + \frac{Q^2}{0.46(GeV/c)^2})$ [129, 130] or $1/(1 + \frac{Q^2}{0.54(GeV/c)^2})$ [131, 132], respectively. There are no measurements on the $G_{\rho(\omega)\to\pi\gamma}(Q^2)$ form factors. However, investigations, one based on QCD sum rules [133] and another one on a quark model [134], predict that the Q^2 dependence of these form factors follows closely the dipole form. Therefore our corresponding background estimations proceed from the assumption that $G_{\rho(\omega)\to\pi\gamma}(Q^2) \sim 1/(1 + \frac{Q^2}{0.71(GeV/c)^2})^2$.
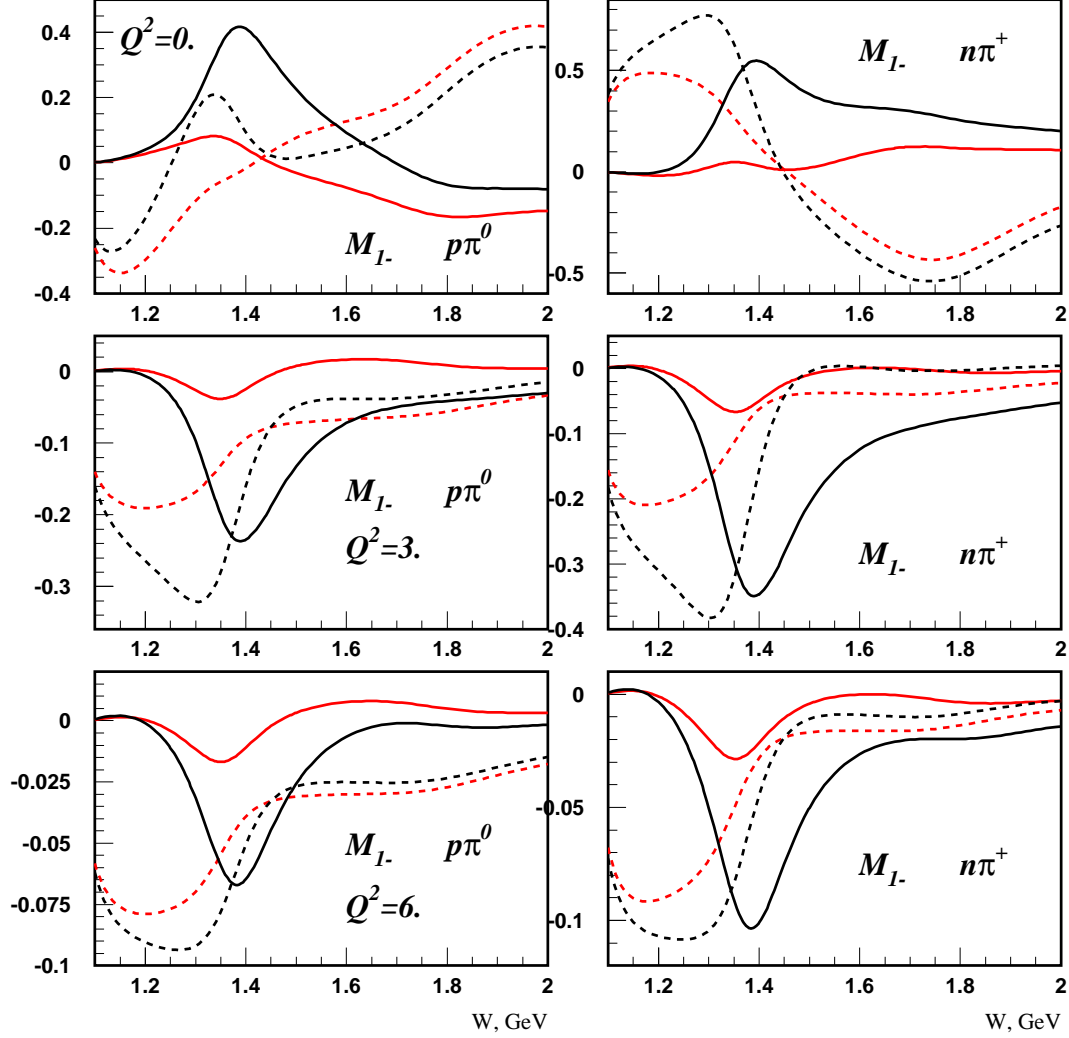
Figure 10: The M_{1-} multipole amplitude for the reactions $\gamma^* p \to p\pi^0$ (left) and $n\pi^+$ (right) at $Q^2 = 0$, 3, and 6 $(GeV/c)^2$. Black curves are the total amplitudes, red curves represent the background; each separated into imaginary (real) part and represented by solid (dashed) curves.

Figure 10 shows the M_{1-} multipole amplitudes for the reactions $\gamma^* p \to p\pi^0, n\pi^+$ at $Q^2 = 0$, 3, and 6 $(GeV/c)^2$. The results for $Q^2 = 0$ and 3 $(GeV/c)^2$ correspond to our

analyses [108, 109], and the results for 6 $(GeV/c)^2$ are based on our extrapolation of the $P_{11}(1440)$ resonance contribution determined at $Q^2 = 1.72 - 4.16$ $(GeV/c)^2$ in the analysis [109] of CLAS $\gamma^* p \to n\pi^+$ data [115]. Whereas the background for $Q^2 = 6$ $(GeV/c)^2$ is based on the information of the form factors listed above. All the uncertainties in the form factors are taken into account, including a 50% uncertainty for $G_{\rho(\omega)\to\pi\gamma}(Q^2)$. All these uncertainties practically do not affect M_{1-} multipole amplitudes and have a very small influence on the background of E_{0+}. From the results presented in Fig. 10, we can draw the interesting and encouraging conclusion that with increasing Q^2 the resonance contributions more visible and stronger in comparison to the background. This behavior of the relative resonances-to-background contributions is connected to the fact that the Q^2 dependence of the background is mainly determined by the proton form factors, which fall as (or stronger than) the dipole form factor, whereas most of resonance amplitudes in the second and third resonance regions seem to fall as $1/Q^3$ driven by the helicity conserving amplitude $A_{1/2}$. The proposed measurement in the Q^2 region from 5.0 to 10 $(GeV/c)^2$ offers therefore a unique and new opportunity to distinguish resonance and background contributions and to investigate the Q^2 evolution of the N^* electrocoupling amplitudes.

5 Isobar model approach for the 2π electroproduction analysis

A comprehensive data set on 2π single-differential fully-integrated electroproduction cross sections measured with CLAS has enabled us to establish the presence and strengths of the essential $p\pi^+\pi^-$ electroproduction mechanisms. This was achieved within the framework of a phenomenological model that has been developed and refined over the past few years by the Jefferson Laboratory - Moscow State University collaboration (JM) [165–173] for analysis of 2π photo- and electroproduction. In this approach the resonant part of the amplitudes is isolated and the Q^2 evolution of the individual electrocoupling parameters of the contributing nucleon resonances are determined from a simultaneous fit to all measured observables.

The mechanisms of 2π electroproduction incorporated into the JM model are illustrated in Figure 11. The full amplitudes are described by superposition of the $\pi^-\Delta^{++}$, $\pi^+\Delta^0$, ρp, $\pi^+ D_{13}^0(1520)$, $\pi^+ F_{15}^0(1685)$, and $\pi^- P_{33}^{++}(1600)$ isobar channels and the direct 2π production mechanisms, where the $\pi^+\pi^- p$ final state is directly created without the formation of unstable hadrons in the intermediate states. Nucleon resonances contribute to the baryon (e.g. $\pi\Delta$) and meson (ρp) isobar channels. The respective resonant amplitudes are evaluated in a Breit-Wigner ansatz, as described in [165]. We included all well established resonance states with hadronic decays into 2 π and an additional $3/2^+(1720)$ candidate state. Evidence for this candidate state was found in the analysis of the CLAS 2π electroproduction data [145].

The $\pi\Delta$ isobar channels are strongest contributors to the 2π electroproduction up to an invariant mass of $W \sim 2.0\,GeV$. They have been clearly identified in the $\pi^+ p$ and $\pi^- p$ single-differential mass distribution cross sections. The non-resonant $\pi\Delta$ amplitudes are calculated from the well established Reggeized Born terms [156, 165, 173]. The initial and final state
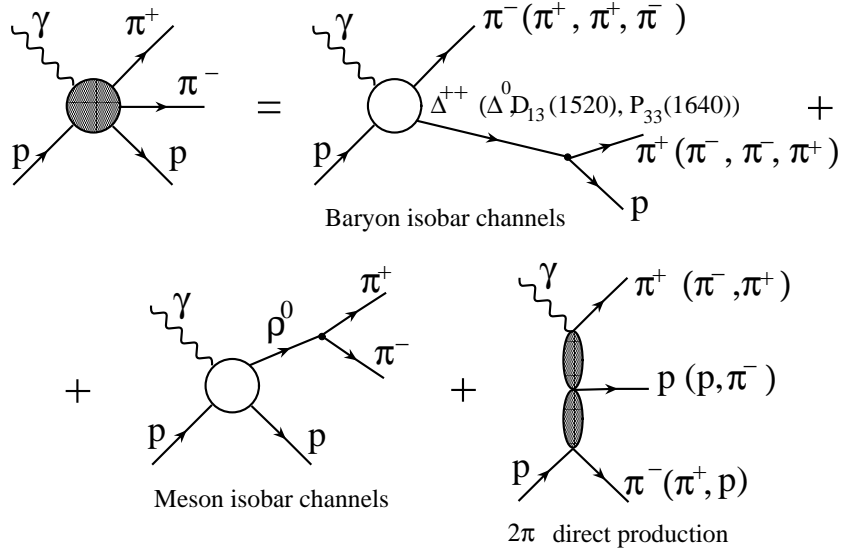
Figure 11: The mechanisms of the JM model.

interactions are described by an effective absorptive-approximation [165]. An additional contact term has been introduced in [169, 171, 173] to account phenomenologically for all remaining possible production mechanisms through the $\pi\Delta$ intermediate state channels, as well as for remaining FSI effects. The parametrization for these amplitudes can be found in [173].

The ρp isobar channel becomes visible in the data at $W > 1.65\,GeV$ with significant resonant contributions for $W < 2.0\,GeV$. Here the non-resonant amplitudes are estimated by a diffractive ansatz, that has been modified in order to reproduce experimental data in the near and sub-threshold regions [170].

The contributions from $\pi^+ D_{13}^0(1520)$, $\pi^+ F_{15}^0(1685)$, $\pi^- P_{33}^{++}(1685)$ isobar channels are seen in $\pi^- p$ and $\pi^+ p$ mass distributions at $W > 1.65\,GeV$. The $\pi^+ D_{13}^0(1520)$ amplitudes are derived from the Born terms of the $\pi\Delta$ isobar channels by implementing an additional γ_5-matrix that accounts for the opposite parity of the Δ with respect to the $D_{13}(1520)$. The amplitudes of $\pi^+ F_{15}^0(1685)$ and $\pi^- P_{33}^{++}(1685)$ isobar channels are parametrized as Lorentz invariant contractions of the initial and final particle spin-tensors and with effective propagators for the intermediate state particles. The magnitudes of all these amplitudes are fitted to the data.

All isobar channels combined account for more than 70% of the charged double pion production cross section in the nucleon excitation region. The remaining part of cross sections stems from the direct 2π production processes, which are needed to describe backward strength in the π^- angular distributions and constrained by the π^+ and proton angular distributions, see Figure 12. The strengths of the direct 2π production mechanisms, shown

23

in bottom row of Figure 11, have been fitted to the CLAS data [145, 147, 148] and can be found in [173].

Within the framework of the JM approach we achieved a good description of the CLAS 2π data over the entire kinematic range covered by the measurements. As a typical example, the model description of the nine single-differential cross sections at $W = 1.51\,GeV$ and $Q^2 = 0.425\,(GeV/c)^2$ are presented in Figure 12 and compared to the contributing mechanisms. Each mechanism has very different qualitative shapes of their cross section contributions in various observables, that are highly correlated by the reaction dynamics. This is the reason why the successful simultaneous description of the nine single-differential cross sections enables us to identify the most essential contributing processes and to access their dynamics at the phenomenological level. On one hand, the extension of this approach to higher $Q^2 10(GeV/c)^2$ will allow us to determine the dynamics of new and still unknown mechanisms, and on the other hand, the amplitudes of various non-resonant mechanisms derived from the JM data fit are a valuable input for N^* studies based on the global multi-channel analysis in a full coupled-channel approach that is currently developed by EBAC [99–101].

The separation of resonant and non-resonant contributions based on the JM model parameters, that have been adjusted to the experimental data, are shown in Figure 13. The differential cross sections underline again the sensitivity of the experimental data to the resonant amplitudes. The resonant part increases relatively to the non-resonant part with W and Q^2. At $W > 1.65\,GeV$ it becomes a largest contribution over a wide range of π^-, π^+ and proton emission angles. Resonant and non-resonant parts have qualitatively different shapes in all observables, allowing us to isolate the resonant contributions and to extract the N^* electrocoupling amplitudes.

An important feature of JM is the capability to pin down the contributing mechanisms from the fit to the experimental data. Therefore, we are planning to use the JM05 model as the general framework for the analysis of the 2π electroproduction data from CLAS12 with the goal to determine the Q^2-evolution of N^* electrocoupling parameters. The key requirement for the proposed experiment is the capability to obtain the full set of nine single-differential $\pi^-\pi^+ p$ final state cross-sections as described and shown above.

6 N* electrocoupling results from single and double meson electroproduction

The CLAS data has enabled us for the first time to determine the $P_{11}(1440)$, $S_{11}(1535)$, and $D_{13}(1520)$ electrocoupling amplitudes over a wide range of photon virtualities by analyzing the two major exclusive channels: 1π and 2π electroproduction. These analyses of the CLAS data have been carried out within the framework of the approaches (DR, UIM, JM) described. The electrocoupling amplitudes of the $P_{11}(1440)$ and $D_{13}(1520)$ states as extracted from 1π and 2π data are shown in Figures 14 and 15. The agreement of the results obtained from the analyses of 1π and 2π channels is both convincing and promising, since the 1π and 2π meson electroproduction channels have completely different non-resonant am-
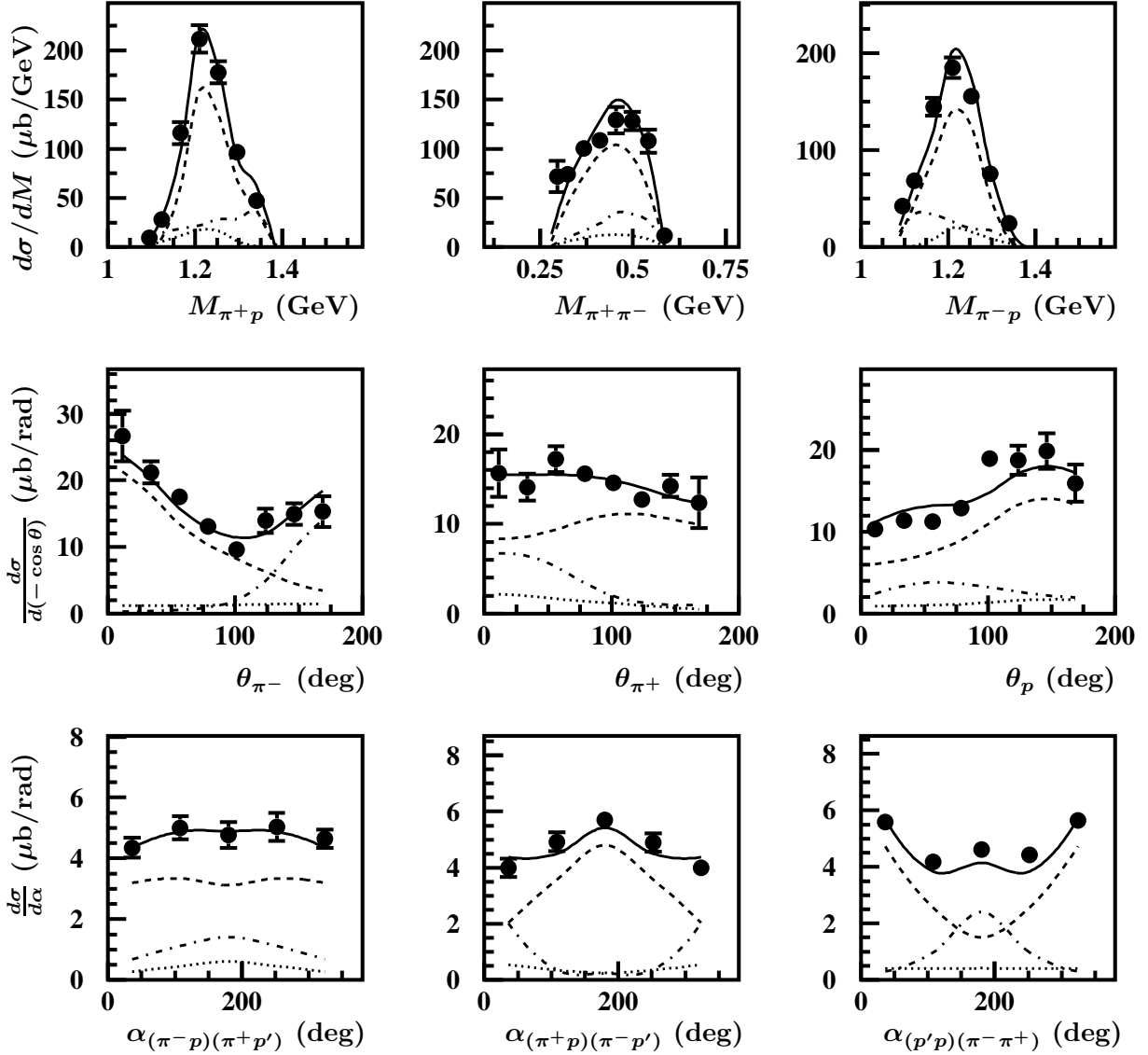
Figure 12: Description of the CLAS charged double pion differential cross sections at $W = 1.51\,GeV$ and $Q^2 = 0.425\,(GeV/c)^2$ within the framework of the JM model. Full calculations are shown by the solid lines. Contributions from $\pi^-\Delta^{++}$ and $\pi^+\Delta^0$ isobar channels are shown by the dashed and dotted lines, respectively, and contributions from the direct charged double pion production processes are shown by the dot-dashed lines.
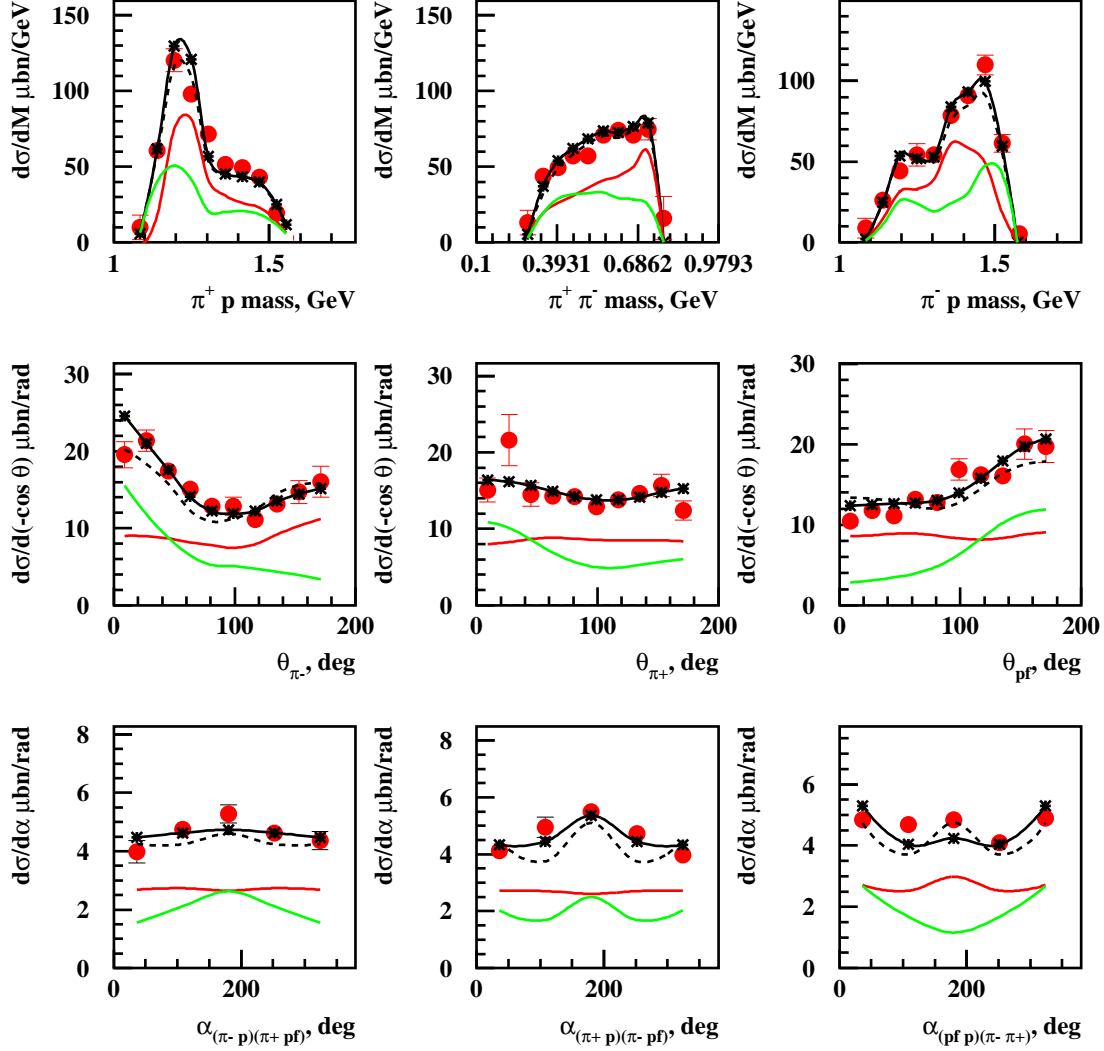
Figure 13: Resonant (red lines) and non-resonant (green lines) contributions to the charged double pion differential cross sections at $W = 1.71\,GeV$ and $Q^2 = 0.65\,(GeV/c)^2$. The full JM calculation is shown by black lines, whereas the solid and dashed lines correspond to two different sets of $A_{1/2}$, $A_{3/2}$ electrocoupling amplitudes for $3/2^+(1720)$ candidate state.
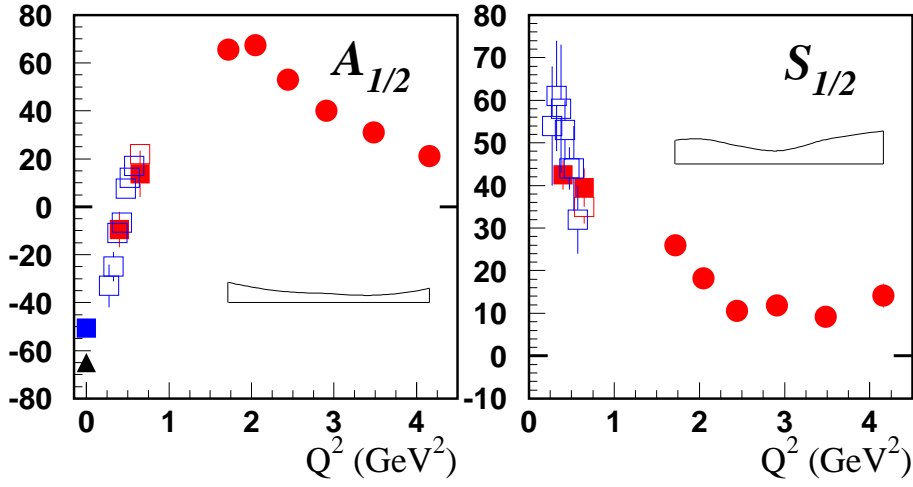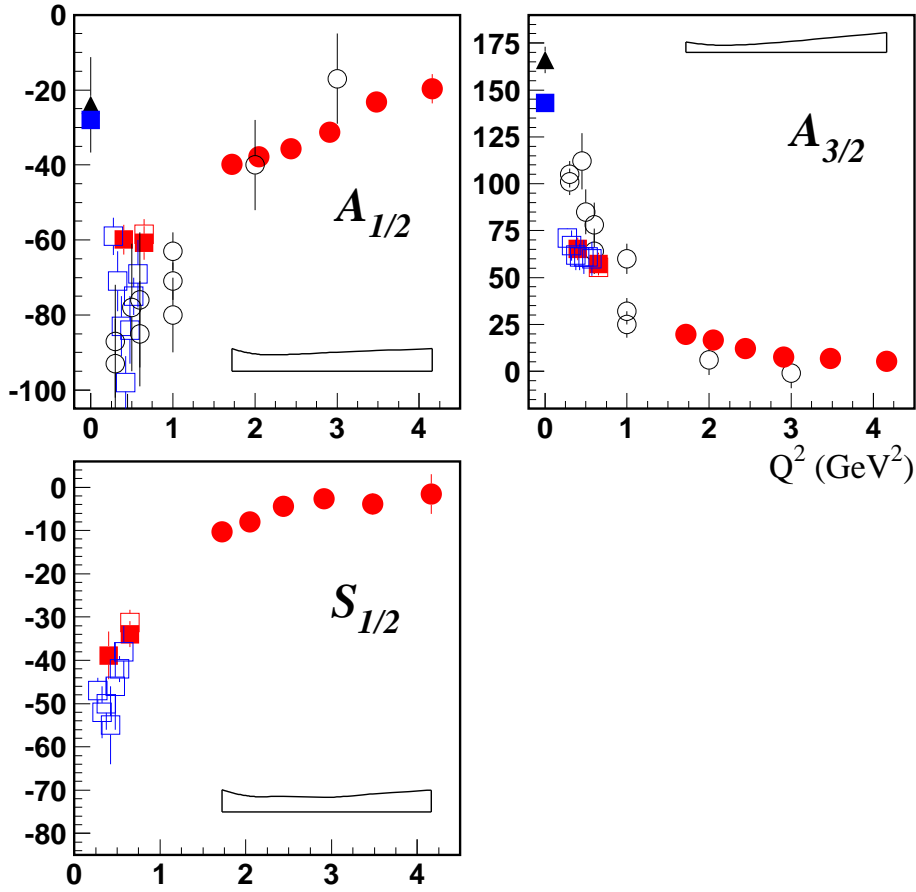
Figure 14: Helicity amplitudes of the $P_{11}(1440)$ electro-excitation of the proton in units of $10^{-3}GeV^{-1/2}$. CLAS analysis results of the CLAS 1π production data are represented by the red circles and squares, while the open squares are for a combined CLAS analysis of the 1π and 2π channel. Preliminary results of the CLAS 2π data at low Q^2 are shown by blue open squares.

plitudes. The successful description of the large body of CLAS and world data on 1π and 2π electroproduction with almost the same values for the $P_{11}(1440)$ and $D_{13}(1520)$ electrocoupling amplitudes, represents compelling evidence for the capability of the described approaches that are utilized by the CLAS Collaboration to provide a reasonable evaluation of the resonance parameters.

The analysis of available CLAS data reveals evidence for substantial modifications of resonance excitation mechanisms at $Q^2 3.0(GeV/c)^2$. Figure 16 shows the $A_{1/2}$ N to N^* transition amplitudes for several low-lying excited states that are scaled by Q^3. At $Q^2 3.0(GeV/c)^2$ the scaled $Q^3A_{1/2}$ amplitude is consistent with a constant behavior for all shown resonances. This is an experimental indication for a transition into a region where the photon interacts primarily with the quark fields in these resonance excitation processes.

Figure 17 shows the electrocoupling amplitudes of two high-lying resonances, $D_{33}(1700)$ and $P_{13}(1720)$ that are extracted from CLAS 2π data within the framework of the JM model and from analysis of the 1π world data available before experiments with CLAS. These two resonances have strong hadronic decays into the 2π channel. The 1π electroproduction channels have not enough sensitivity to these states, which explains the large uncertainties of the world data on $D_{33}(1700)$ and $P_{13}(1720)$ helicity amplitudes. Studies of the 2π electroproduction data from CLAS have enabled us for the first time to map out their Q^2-evolution with significantly higher precision. The 2π electroproduction channel hence offers a very promising alternative to study higher-lying resonances ($W > 1.65GeV$). The majority of these states decay dominantly by 2π emission. The combined analysis of 1π and 2π elec-

troproduction opens an excellent opportunity to access electrocoupling amplitudes of the excited proton states with even higher precision. The shown results obtained from 1π and 2π CLAS data analyses represent reasonable, initial estimates of the Q^2 evolution of the N^* electrocoupling amplitudes. This information will be checked and improved in by a global and complete coupled-channel analysis that incorporates a broader base of non-resonant amplitudes extracted from the CLAS data by the phenomenological models described above. This program forges important joint effort between Hall B and EBAC at Jefferson Lab.

Figure 15: Helicity amplitudes of the $D_{13}(1520)$ electro-excitation of the proton in units of $10^{-3}GeV^{-1/2}$. CLAS analysis results of the CLAS 1π production data are represented by the red circles and squares, while the open squares are for a combined CLAS analysis of the 1π and 2π channel. Preliminary results of the CLAS 2π data at low Q^2 are shown by blue open squares, World data results of 1π electroproduction, available before CLAS, are represented by black open circles.
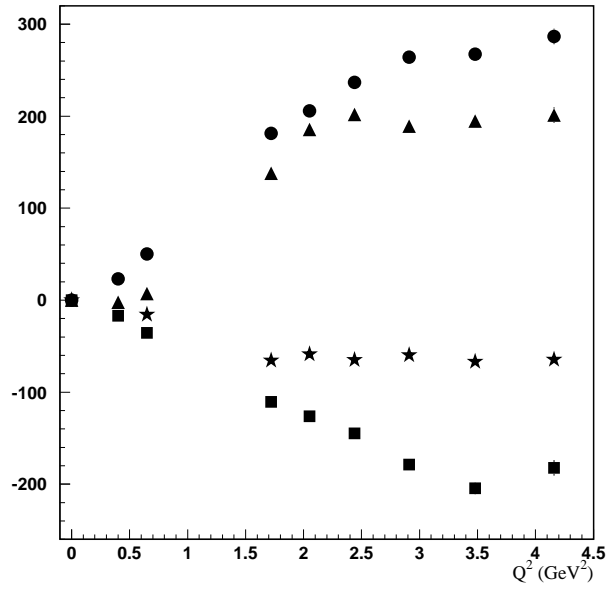
Figure 16: The $A_{1/2}(Q^2)$ helicity amplitudes are scaled by $Q^3/1.0\ (GeV/c)^2$ and shown for the Roper $P_{11}(1440)$ (triangles), $S_{11}(1535)$ (circles), $D_{13}(1520)$ (squares), and $F_{15}(1680)$ (stars). At the highest currently accessible momentum transfers the Q^2 dependence is consistent with a flat behavior.

30
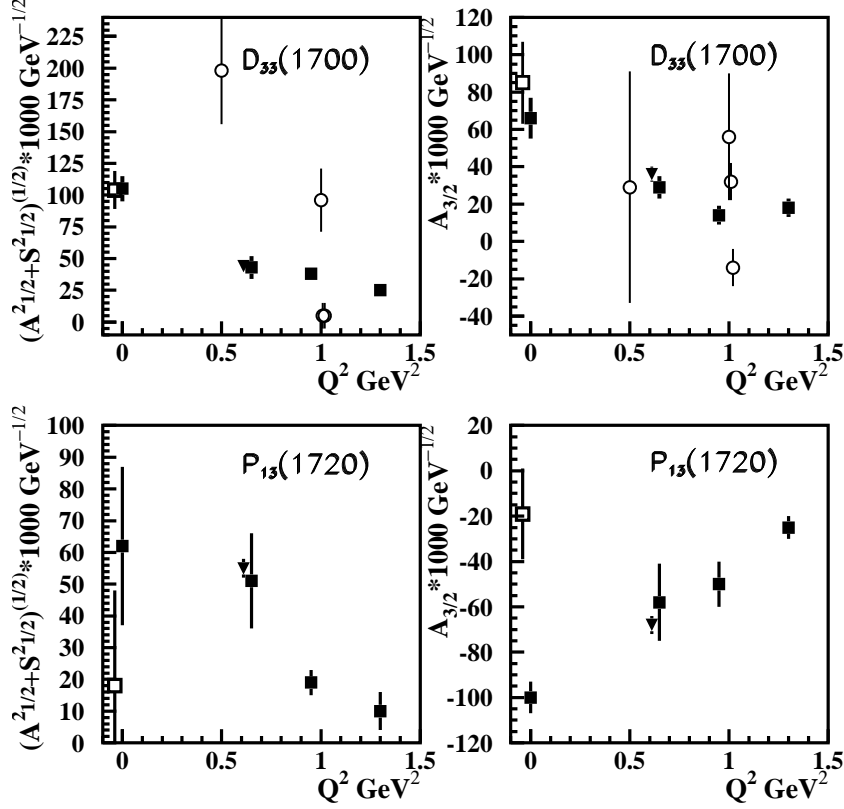
Figure 17: Helicity amplitudes for the electro-excitation of $D_{33}(1700)$ and $P_{13}(1720)$ on proton in units of $10^{-3}GeV^{-1/2}$. Results from the CLAS 2π production data analysis are shown as filled squares and triangles represent the combined analysis results of 1π and 2π channel [108]. World results from the 1π data analysis are shown as open circles.

7 Double-Charged Pion Electroproduction Experiment

7.1 Experimental studies of 2π photo- electro-production in N^* excitation region

The available data on 2π production by real and virtual photons have already provided a considerable amount of information for the evaluation of N^* electrocoupling amplitudes at photon virtualities Q^2 below 1.5 GeV^2. They consist of old bubble chamber measurements [186] at the photon point and recent real photon data collected at ELSA, GRAAL, and MAMI [177–180, 182–185]. The most detailed charged 2π electroproduction data have been obtained with the CLAS detector [145, 147, 148]. These data cover a kinematic range in W from 1.3 GeV to 1.9 GeV and for photon virtualities Q^2 from 0.2 GeV^2 to 1.5 GeV^2. Fully integrated 2π electro-production cross section data measured with CLAS are shown on Figure 19.
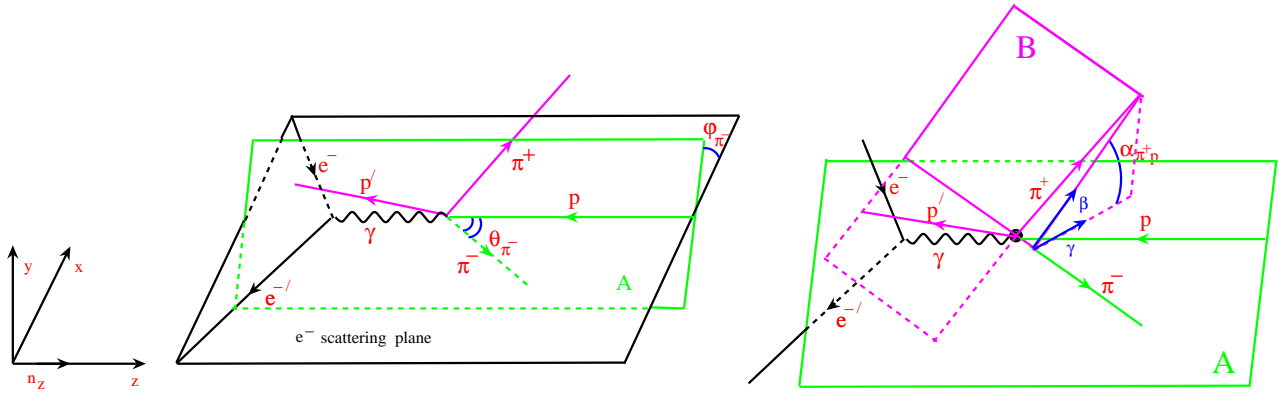
Figure 18: Angular variables used in the analysis of the 2π production CLAS data.

The description of the $\pi^-\pi^+p$ final states requires five kinematic variables, which may be chosen to be two invariant masses of the final hadrons, the solid angle describing the momentum of one of the hadrons, and the angle between two planes. The three-momenta of two pairs of the final hadrons are chosen to define these two planes. The choice of the five variables is not unique. The angular variables used in the CLAS analysis are shown in Figure 18. In each covered (W, Q^2) bin, the following single differential cross-sections integrated over the 4 other variables are obtained:

- $\pi^-\pi^+$, π^+p, π^-p mass distributions

- π^+, π^-, p CM-angular distributions

- 3 distributions over the angles between two planes, composed by two pairs of 3-momenta of the final hadron for 3 possible combinations of hadron pairs, see for example α in Figure 18.
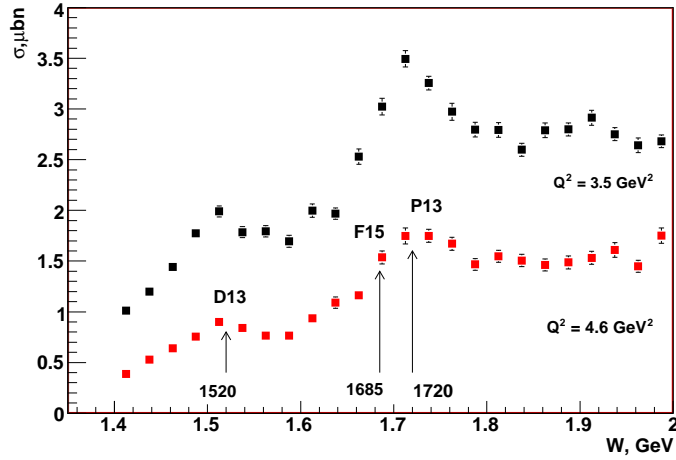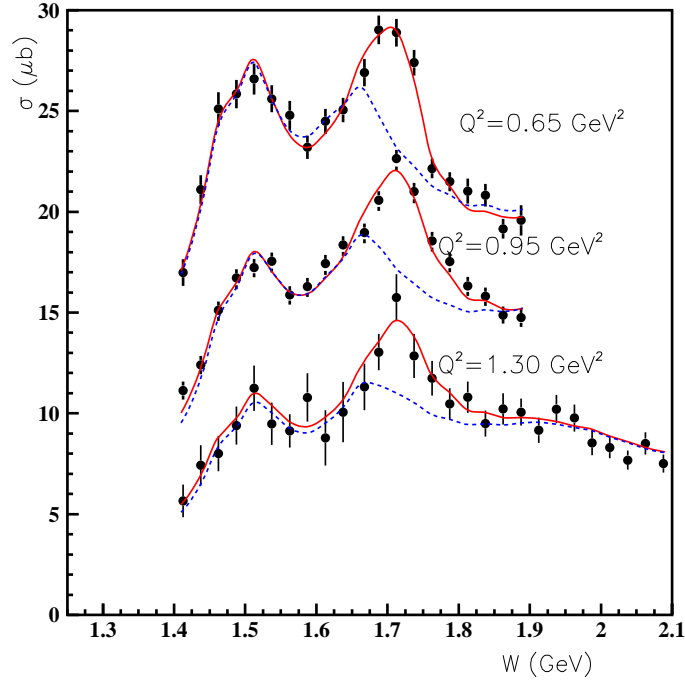
32

Figure 19: Total double charged pion virtual photon cross-sections at $Q^2 < 1.5 \ GeV^2$ (top) [145] and at high Q^2 form 3.0 to 5.0 GeV^2 (bottom) [146]. The fit of CLAS data [145] within the framework of the JM model [167] is shown by solid lines. The dashed lines correspond to the JM05 calculation without the $3/2^+(1720)$ candidate state.

A detailed set of measurements of unpolarized observables is available for the first time from the CLAS detector, that has an acceptance of close to 4π. Examples of measured sets

of nine single-differential CLAS cross sections are shown in Figures 12 and 13. A similar set of measurements can be expected with CLAS12. It is a considerable advantage for the analyzing of the $\pi^+\pi^-p$ final state data to have all nine single-differential cross sections in each (W, Q^2) bin. The total $\pi^-\pi^+p$ cross sections calculated with the framework of JM05 model [?] is shown in comparison with CLAS data [145, 146] on the left panel of Figure 19, and preliminary CLAS data at high photon virtualities are shown in the right panel of Figure 19. Resonance structures are clearly visible in the 2π electroproduction data over the entire Q^2 range covered by the CLAS measurements.

7.2 Feasibility of N^* studies by 2π electroproduction at high photon virtualities

Based on the successful extraction of the electrocoupling amplitudes for various excited proton states from the available CLAS 2π data within the JM model, we propose to extend this extraction of the Q^2 evolution of the N^* electrocoupling amplitudes photon virtualities that become accessible with the 11 GeV electron beam, if:

- the collected statistic will be comparable to the one that we have reached with CLAS, and

- the ratio of resonance over non-resonance contributions will be comparable or better than in already studied region of Q^2.

First we evaluate the resonant to non-resonant contribution ratio at photon virtualities beyond those covered by the available CLAS 2π measurements. These calculations have been carried out within the framework of JM03 version [167?] for Q^2s from 1.5 to 4.0 GeV^2. For this extrapolation we used the JM03 version with a 3-body phase space parametrization for all remaining processes, that was fitted to the CLAS 2π data and extrapolated to higher Q^2 by using a second order polynomial for the Q^2 evolution. These calculations showed that Q^2 evolution of non-resonant amplitudes may be well described by power dependence proportional to Q^{-n}, with n in a range from 3 to 4. The $A_{1/2}$ resonant amplitudes, that are leading at high Q^2 evolve proportional to Q^-3, as indicated in Figure 16. At photon virtualities above 1.0 GeV^2 the ratio of resonant to non-resonant amplitudes remains therefore either unchanged with Q^2 or increases in our favor. These JM model predictions are consistent with the observation of resonant structures in fully integrated 2π production cross sections at the highest Q^2 currently accessible at JLab, as shown in Figure 19. We thus concluded that the ratio of resonant over non-resonant contributions at high Q^2 will at least be not smaller than the one extracted from the CLAS data at photon virtualities lower than 1.5 GeV^2. The N^* electrocoupling amplitudes at Q^2 from 5.0 to 10.0 GeV^2 can thus be determined, if the statistics collected in each (W, Q^2) bin and the acceptance coverage by of CLAS12 will be comparable or better than for CLAS [145],[147, 148].

7.3 Simulation of 2π electroproduction in CLAS12

We carried out the studies of resolution and acceptance of the CLAS12 detector with a goal to evaluate our capabilities to obtain double charged pion electroproduction cross sections in the Q^2 range from 5.0 to 10 GeV^2. In simulation we used Genova event generator [187]. For an electron beam energy of 11 GeV, we simulated 2 pion and 3 pion electroproduction channels. The CLAS Fast MC package [188] has been used to simulate the CLAS12 response to the generated events. Generated and accepted events have been studied over the full proposed kinematic range, W from 1.2 to 3.5 GeV and Q^2 from 5.0 to 10.0 GeV^2. For the accepted 2π events we applied selection procedures and kinematic cuts similar to those already used in the analysis of available CLAS 2π data.

Fist, we studied the capability to isolate a sample of 2π events within a multi-pion electroproduction data set. The distribution over $M^2_{\pi^+ pX}$ missing mass squared for 2 pion and 3 pion events are shown on Figure 20, accounting for all momentum smearing expected for CLAS12.
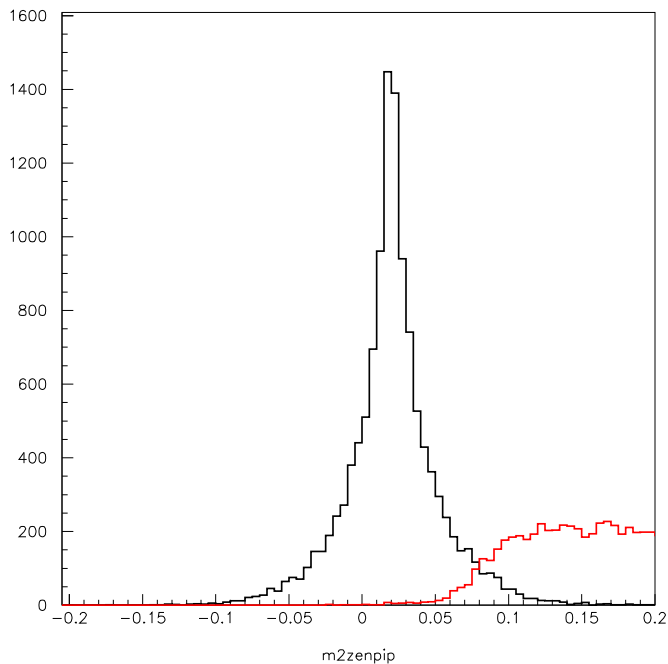
Figure 20: Distributions of $M^2_{\pi^+ pX}$ for detected 2π (black) and 3π events (red) curves.

Applying a $M^2_{\pi^+ pX} < 0.07\ GeV^2$ cut will ensure a good isolation of 2π events with only few percents multi-pion contamination. The quality of the multi-pion background rejection may be further improved, if we restrict the W range to $< 2.0 GeV$, which corresponds to the major part of conventional N^*s. Another way to improve multi-pion rejection is to exploit the correlation between squared missing masses $M^2_{\pi^+ \pi^- pX}$ and missing energies for the $\pi^- \pi^+ p$ final hadronic system. But we need to detected all 3 final hadrons to apply this

35

method. The $M^2_{\pi^+\pi^- pX}$ vs. missing energy correlation is shown in Figure 21 for 2 and 3 pion events. 2π events are accumulated in the spot around zero, whose size is determined by the mass and energy resolution. 3 pion events accumulate in the vertical strip along the missing energy direction. The 2π event separation is pretty good, however this technique reduces the efficiency.
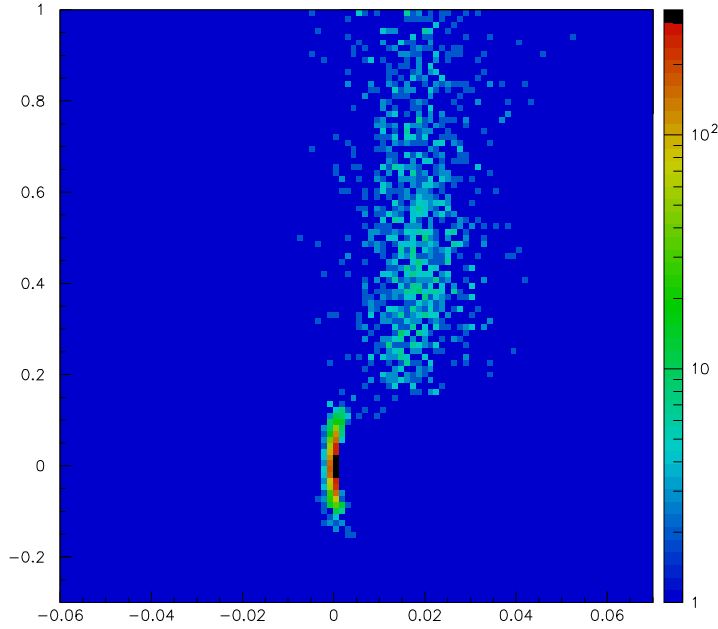

Figure 21: Separation of 2π events from the multi-pion background, using the missing energy - $M^2_{p\pi^+\pi^- X}$ kinematic correlation, with 2π events in the spot around zero and 3 pion events in the vertical strip.

We carried out efficiency evaluation for measurements of 2π events with CLAS12. Estimated in MC simulation efficiency for detection of 2π events, when all three final hadrons are detected is shown on Fig. 22. Efficiency is rather uniform in $(Q^2\,\&\,W)$ plane with average value 20 %. This value of efficiency was used in evaluation of counting rate.

On Fig. 23 and Fig. 24 we show efficiency for various $\pi^+\pi^- p$ final state kinematics variables. All these efficiencies were averaged over other 4 kinematics variable for $\pi^-\pi^+ p$ final state. Efficiencies were estimated in W interval from 1.5 to 1.7 GeV and averaged over photon virtualities from 5.0 to 10.0 GeV^2. Top and middle rows on Fig. 23 and Fig. 24 are generated and accepted events respectively, while efficiencies are shown at the bottom rows.

Efficiencies for various final state hadronic variables are rather flat. So, even simplest event generators may be used to estimate efficiencies in real data analysis.

Momentum resolution for final hadron are shown on Fig. 25, Fig. 26 and Fig. 27. The $(p_{rec} - p_{gen})/p_{gen}$ distributions at various particle momenta are shown. Here p_{rec} and p_{gen} stand for momenta of reconstructed and generated hadrons respectively. Momentum res-
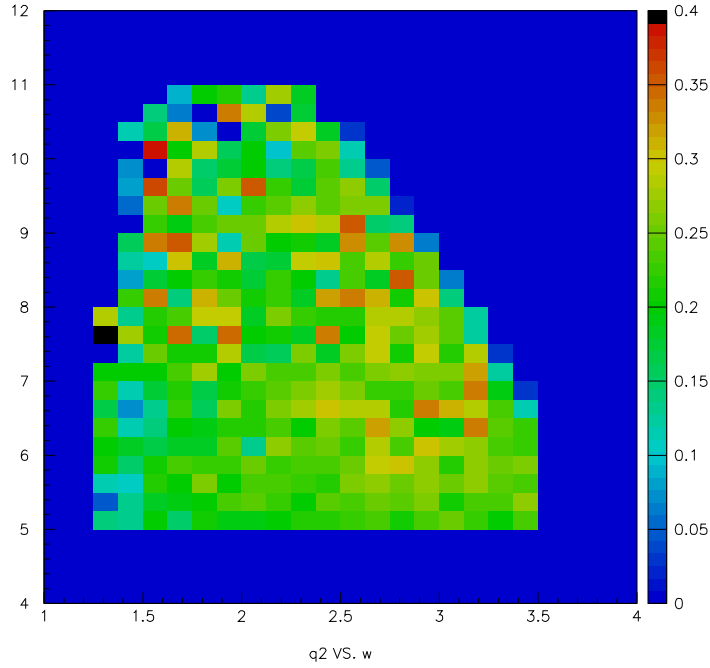
Figure 22: Efficiency for detection of 2π events with CLAS12 in the (Q^2, W) plane for $\pi^+\pi^- p$ detected

olution ranges within several percents for FWHM and rather independent from particle momenta.

Using expected final particle momentum smearing for CLAS12, we estimated W-resolution, averaged over W from 1.3 to 2.0 GeV and Q^2 from 5.0 to 10 GeV^2. Calculations were carried out for two possible ways to determine W from data. First, W may be estimated from electron scattering kinematics. W resolution achieved in this way is shown on Fig. 28 as selected 2π event distribution over value $(W_{rec} - W_{gen})/W_{gen}$. Here W_{rec} and W_{gen} stand for W of reconstructed and generated events respectively.

W resolution at W range from 1.5 to 2.0 GeV is 1.5% σ value or 3.3% FWHM. This resolution improves as W increases. However for W=1.7 GeV 3.3% FWHM corresponds to almost 60 MeV absolute value for resolution. It is comparable with total hadronic decay width of N^* in this mass range. So we tried to figure out a way to improve W resolution. We studied another possibility to determine W from four-momenta of the final hadrons. Absolute value of the final hadron momenta are defined by W. So, at $W < 2.0$ GeV absolute value for hadron momenta smearing should me much less, then for scattered electron of 7-10 GeV momenta, corresponded to N^* excitation. Therefore, we may expect improvement in W-resolution, if W value would be calculated from the final hadron momenta. W resolution achieved in this way is shown on Fig. 29 For W from 1,3 to 2.0 GeV we have considerable improvement. FWHM fall down from 3.3% to 0.6%.

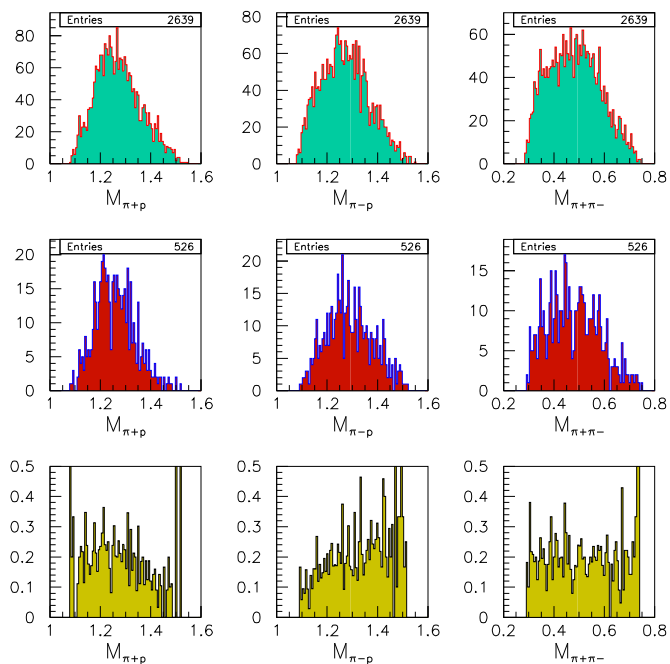So, we are going to determine W value from three momenta of the final hadrons. In this

Figure 23: Efficiencies for various mass distributions in 2π production averaged over W from 1.5 to 1.7 GeV and Q^2 from 5.0 to 10.0 GeV^2. The distributions for generated and accepted events are shown in the top and middle row, respectively. The estimated efficiencies are presented in the bottom row.

case we may adopt size of W-cell 25 MeV. This size of W-cell was used for evaluation of counting rate, while size over Q^2 was determined by requirement to collect proper statistic during experimental run and chosen equal to 0.5 GeV^2.

To estimate counting rate, we need some evaluation for double charged pion cross-sections at Q^2 from 5.0 to 10.0 GeV^2. In this kinematics area we unable to use JM model, since at this high photon virtualities Q^2 evolution of non-resonant processes may be considerably different than expected from extrapolation of the non-resonant amplitudes derived from the data fit at $Q^2 < 1.5 GeV^2$. So, we accepted another approach for indicative estimates of total 2π cross-sections. As a starting point we used fit of inclusive structure function proposed in [189]. This fit works pretty good at $Q^2 < 10.0$ GeV^2 in N^* excitation region. From this fit we estimated total inclusive virtual photon cross-section off protons. To obtain 2π total cross-sections, we used ratio 2π cross-section over inclusive virtual photon cross-section. This ratio was taken from CLAS data at $Q^2 < 1.5 GeV^2$ and extrapolated to the Q^2 area from 5.0 to 10.0 GeV^2. Estimated in this way total 2π cross-sections at several W values are shown on Fig. 30.

We used average efficiency value for detection of 2π events 20%, estimated with CLAS12 Fast MC.

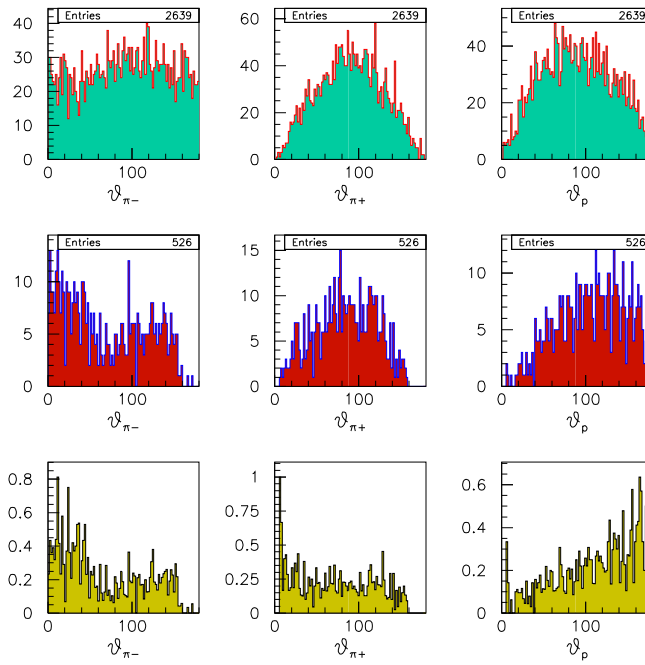The number of collected events as described above (Q^2&W) cells is shown on Fig. 31 for

Figure 24: Efficiency for various angular distributions in 2π production averaged over the four other kinematics variables at W from 1.5 to 1.7 GeV and at Q^2 from 5.0 to 10.0 GeV^2. The distributions for generated and accepted events are shown in the top and middle row, respectively. The estimated efficiencies are presented in the bottom row.
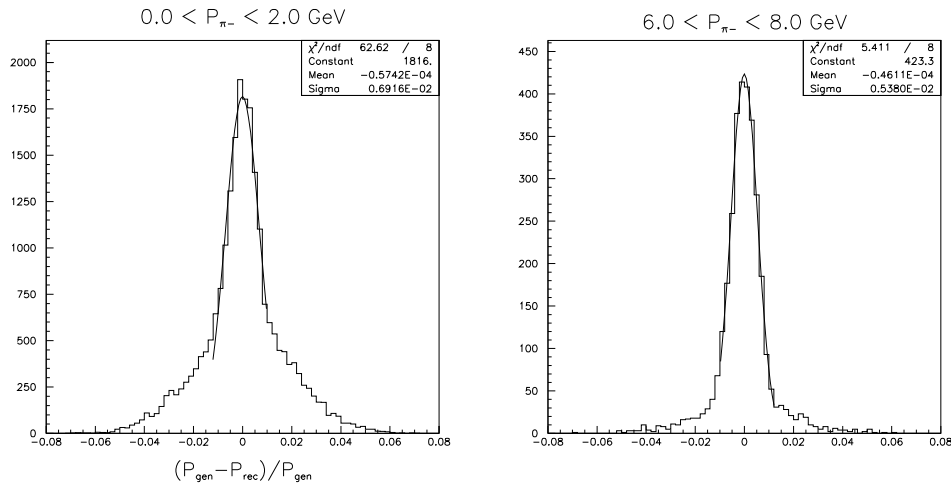

Figure 25: Momentum resolution for π^-. p_{rec}, p_{gen} are momenta for reconstructed and generated particle respectively.
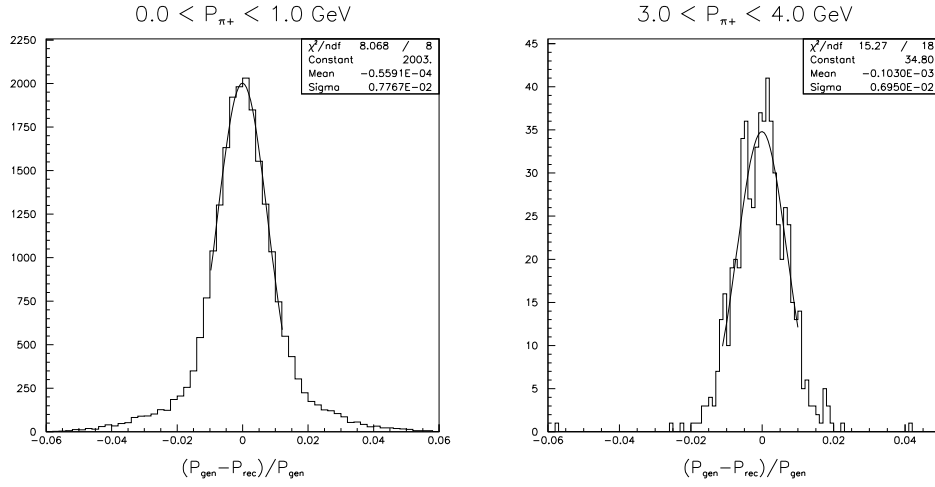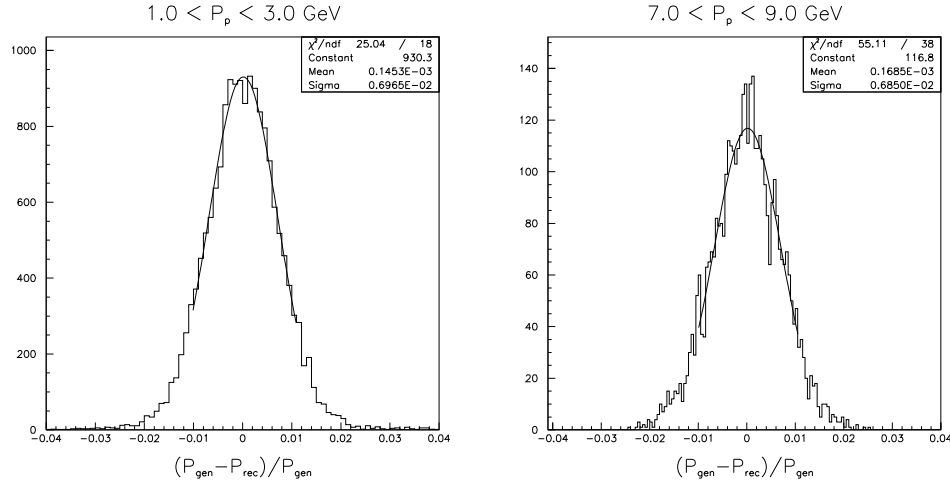
60 days run time.

Figure 26: Momentum resolution for π^+. p_{rec}, p_{gen} are momenta for reconstructed and generated particle respectively.

Figure 27: Momentum resolution for protons. p_{rec}, p_{gen} are momenta for reconstructed and generated particle respectively.

In analysis of available CLAS 2π data [145, 147, 148] we needed statistic above 10000 events for most $(Q^2 \& W)$ cells, to obtain entire set of 2π single differential cross-sections, described in Section 7.1.1. As it follow from Fig. 31, counting rate for 2π events with CLAS12 will be sufficient to produce cell population >10000 2π events in W area from 1.7 to 1.9 GeV and likely in overall N^* excitation region, based on available data both on W-dependence of 2π integrated cross-sections and inclusive structure functions.
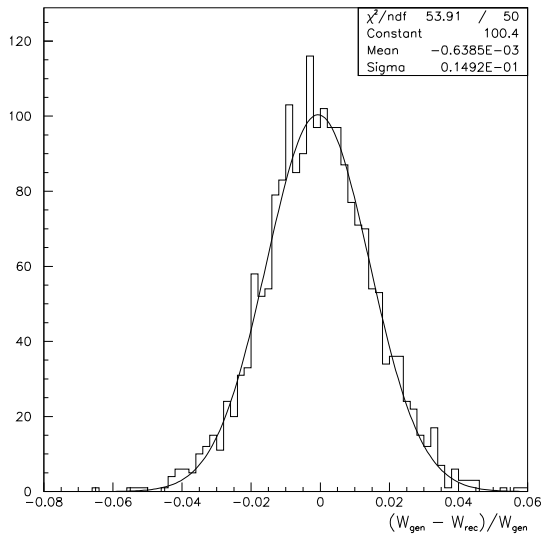
Figure 28: Resolution over W, averaged over W from 1.5 to 2.0 GeV and over photon virtualities from 5.0 to 10 GeV^2. Invariant mass of the final hadronic system were determined from electron scattering kinematics.
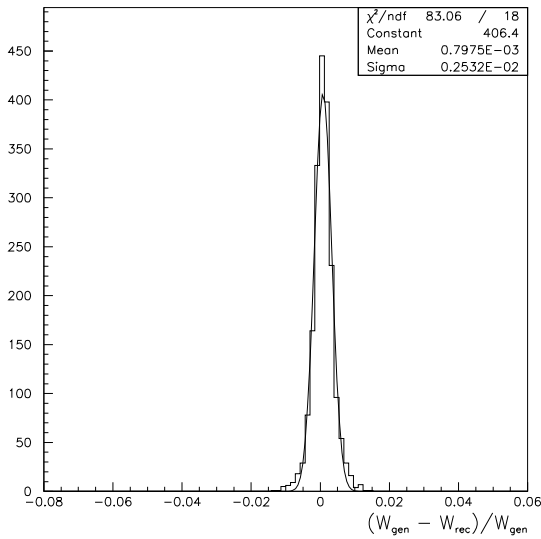

Figure 29: The same as on Fig. 28. Invariant masses of the final hadronic system were determined from the final hadron momenta.
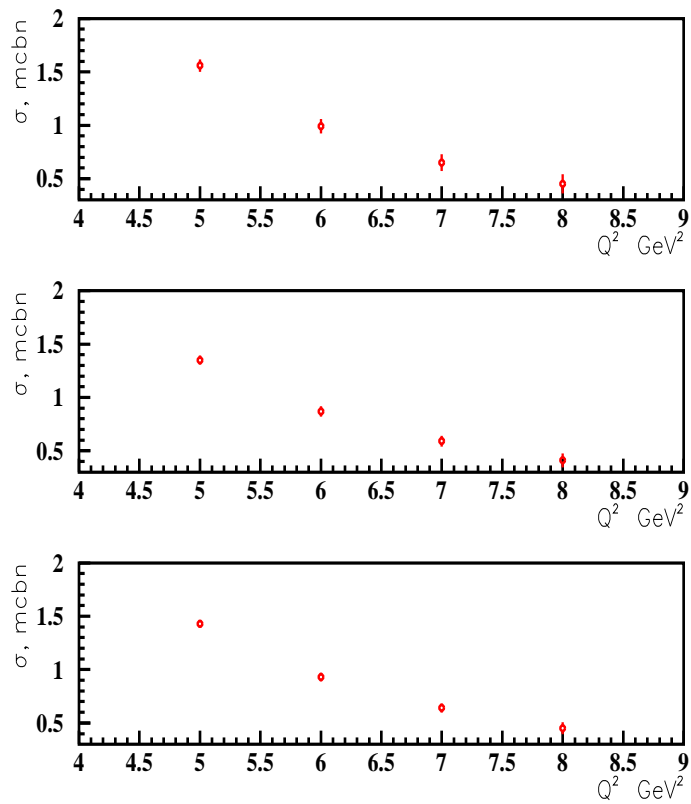
41

Figure 30: Total 2π cross-sections at photon virtualities from 5.0 to 10.0 GeV^2, estimated from the data on inclusive structure function F_2 [189]. W=1.71 GeV (top), W=1.84 GeV (middle), W=1.89 GeV (bottom)
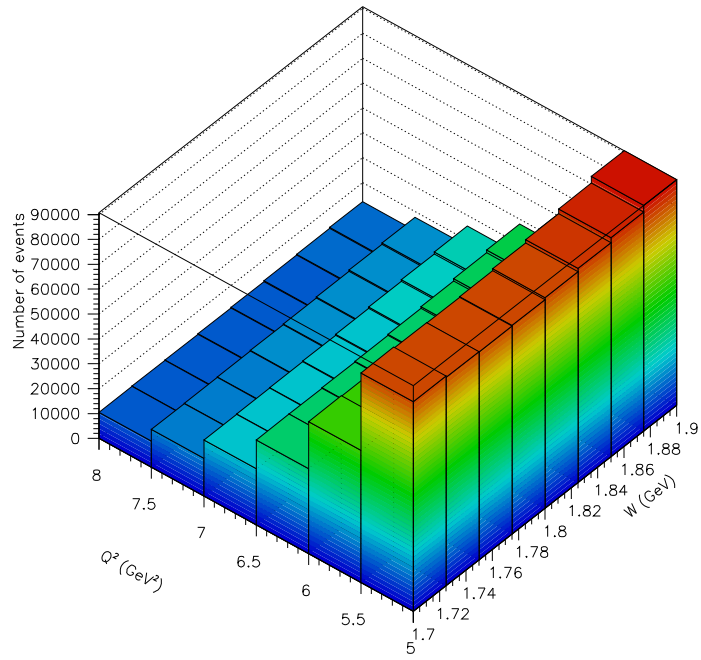
Figure 31: Number of collected 2π events in N^* excitation region with CLAS12. 60 days run time. $10^{35}\,cm^{-2}s^{-1}$ luminosity.

8 Single-Meson Electro-Production Experiment

8.1 Cross Section Measurement and Beam Time Estimates

We propose to extend the measurements of experiment E99-107 to $11\,GeV$ electron beam energy. In the conventional resonance region ($W \leq 2\,GeV$) the covered Q^2 range will extend beyond $12\,GeV^2$ (see Fig. 32). The differential cross section will be measured with a polarized electron beam as a function of the invariant mass W, the azimuthal hadronic angle ϕ_π, and the polar hadronic angle θ_π of the pion nucleon final-state [1]. In the one-photon-exchange approximation the fivefold differential cross section factorizes into the hadronic and the leptonic part [2]

$$\frac{d^5\sigma_v}{dk_{20}^\diamond d\Omega_e^\diamond d\Omega_\pi} = \Gamma_v \cdot \frac{d^2\sigma_v}{d\Omega_\pi}. \tag{1}$$

The virtual photon flux can be written as

$$\Gamma_v = \frac{\alpha}{2\pi^2} \frac{k_{20}^\diamond}{k_{10}^\diamond} \frac{k_\gamma^\diamond}{Q^2} \frac{1}{1-\varepsilon} \tag{2}$$

with the four momentum transfer $K^\mu = K_1^\mu - K_2^\mu$, the corresponding squared four momentum transfer $-K_\mu K^\mu = Q^2$, and the incoming $K_1^\mu = \{k_{10}, \vec{k}_1\}$ and outgoing $K_2^\mu = \{k_{20}, \vec{k}_2\}$ electron four momenta, the equivalent photon energy

$$k_\gamma^\diamond = \frac{s - m^2}{2m} = \frac{W^2 - m^2}{2m} \tag{3}$$

and finally the degree of transverse polarization

$$\varepsilon = \left(1 + 2\,\frac{|\vec{k}^\diamond|^2}{Q^2}\,\tan^2\frac{\theta_e^\diamond}{2}\right)^{-1}. \tag{4}$$

In out-of-plane measurements the specific ϕ_π-dependences of the twofold hadronic cross section

$$\frac{d^2\sigma_v}{d\Omega_\pi} = \sigma_T + \epsilon\sigma_L + \epsilon\sigma_{TT}\cos 2\phi_\pi + \sqrt{\epsilon(\epsilon+1)/2}\,\sigma_{TL}\cos\phi_\pi + \tag{5}$$
$$P_e\sqrt{\epsilon(1-\epsilon)/2}\,\sigma_{TL'}\sin\theta_\pi\sin\phi_\pi$$

can be utilized to separate the four response functions, $\sigma_T + \epsilon\sigma_L$, σ_{TT}, σ_{TL}, and $\sigma_{TL'}$. A separation of σ_T and σ_L is not required for this proposal as the resonance couplings are known to be mostly transverse, thus the longitudinal amplitudes can be extracted with greater sensitivity from the interference terms σ_{TL} and $\sigma_{TL'}$ than from the total cross section. The specific θ_π-dependences of these four response functions on the other hand determine in the covered kinematic region the W and Q^2 evolution of the Legendre moments, which are the basis of the single-pion multipole or helicity amplitude analysis as described in chapter **??**
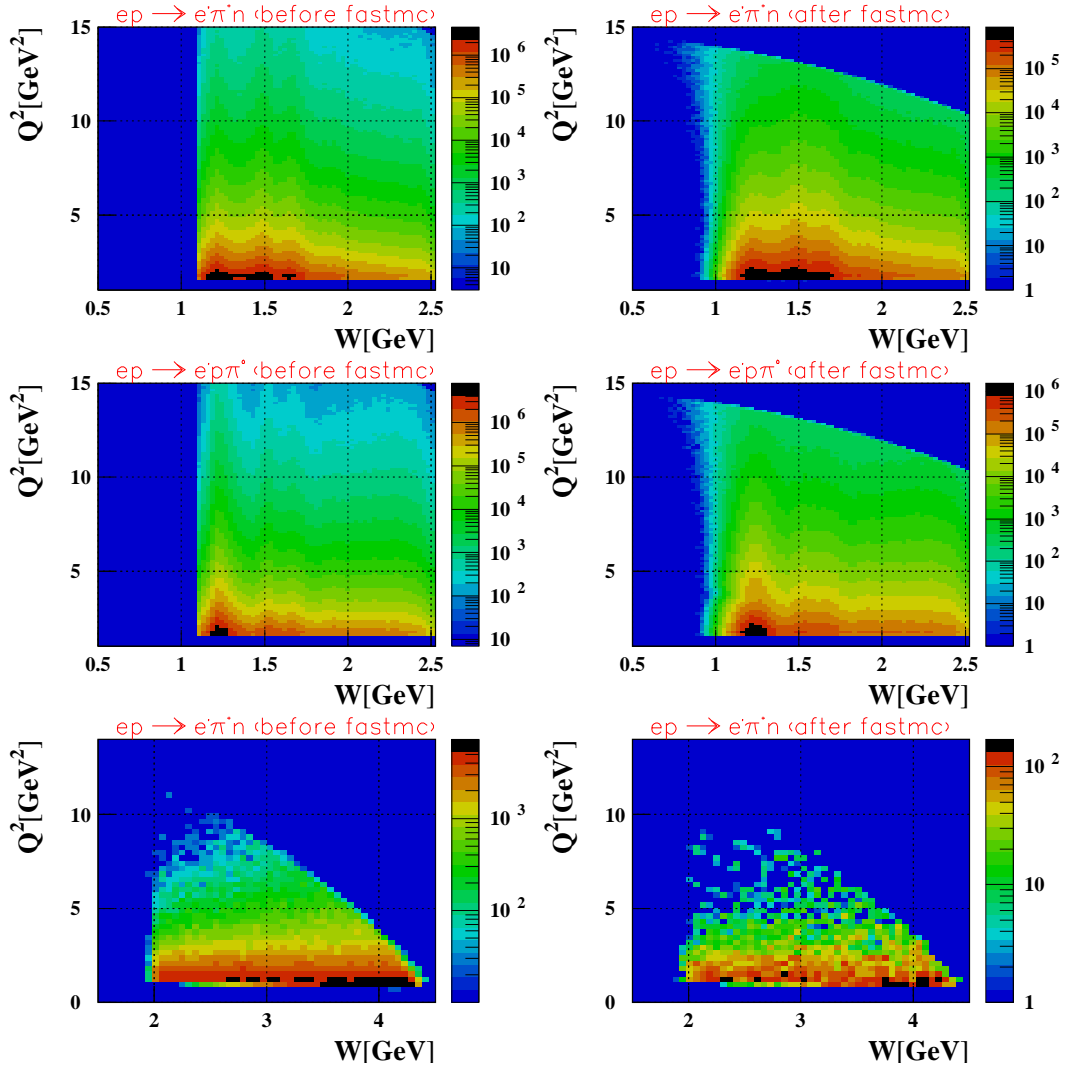
Figure 32: Kinematic coverage of CLAS12 in the resonance region for the exclusive one pion electro-production at $11\,GeV$ electron beam energy when e' and π^+ (upper and lower right panels) or e' and p (middle right panel) are detected in the CLAS12 fastmc simulation based on the Genova-EG (in the resonance region) or DIS (beyond the resonance region) event generator, and the corresponding Genova-EG (upper and middle left panels) and DIS (lower left panel) event generator data itself.

The beam time estimate for the $\gamma^* p \to \pi^+(n)(\pi^0 p, \eta p)$ reaction channel is not only based on the Genova-EG event generator [187] and the CLAS12 fastmc detector simulation, but also

---

[1] The described cross section decomposition applies more generally to any single-meson nucleon final-state.

[2] Variables in the lab frame (LAB) are marked with diamonds $\diamond$ and all unmarked variables are in the center-of-mass frame (CM).
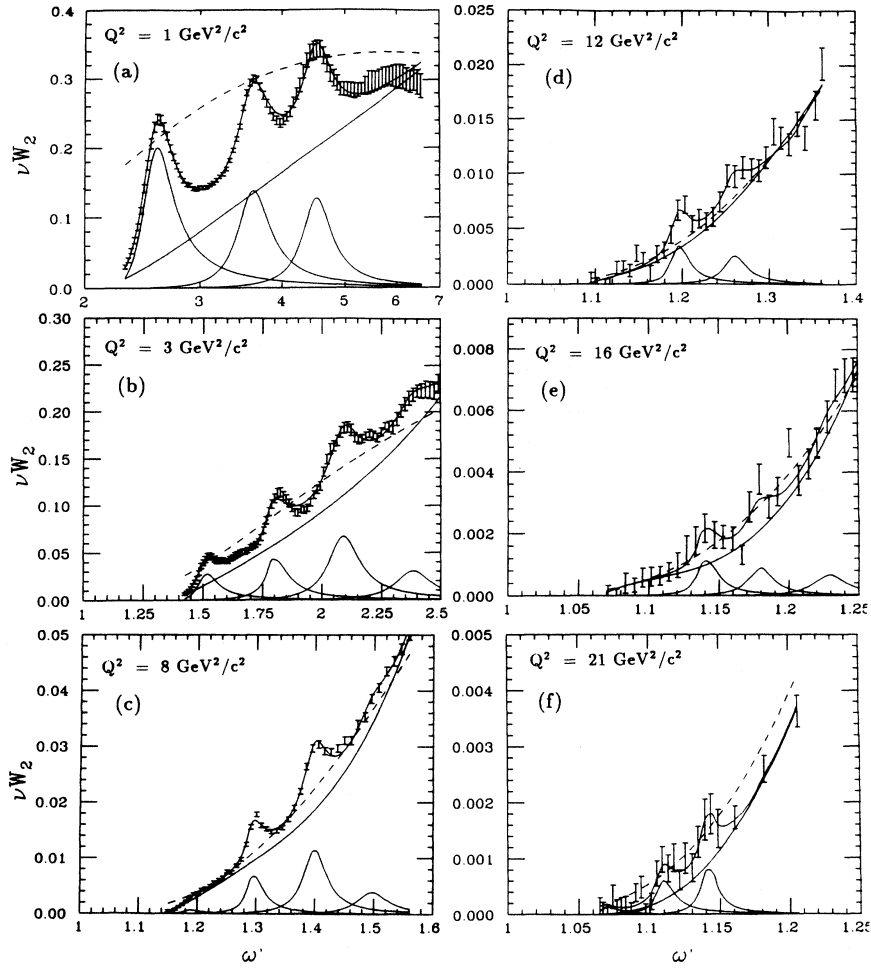
Figure 33: The structure function νW_2 versus ω' inclusive inelastic scattering in the resonance region for various values of nominal Q^2, where $\omega' \equiv 1 + W^2/Q^2$ [? ? ? ? ?]. The solid curves are fits to the data that include only $\Delta(1232)$, $S_{11}(1535)$, and $F_{15}(1680)$ resonance contributions [?]. The dashed curves are fits to the data in the scaling region extrapolated down to the resonance region.

on the measured exclusive [?] and inclusive [?] cross sections. An overview of the inclusive inelastic scattering in the resonance region, as in Fig. 33, demonstrates that at all Q^2 even up to $21\,GeV^2$ resonance structures are visible and that the νW_2 structure function result at $Q^2 = 3\,GeV^2$ agrees with the recent total inclusive cross section at $Q^2 = 2.915\,GeV^2$ [?]. In addition the peak strength in the second resonance region attributed to the $S_{11}(1535)$ and in the third resonance region attributed to the $F_{15}(1680)$ scale like the dipole form factor given by $G_{dip} = \mu_p(1 + Q^2/0.71)^{-2}$ [?]. This experimental result justifies the use of the Genova-

EG event generator beyond the first resonance region, since it also assumes dipole behavior for the Q^2 evolution of the transition form factors. The appropriate [3] normalization of the simulated and acceptance corrected total number of events for $11\,GeV$ electron beam energy to the measured one for $5.75\,GeV$, both at $Q^2 = 3\,GeV^2$, accomplishes a more precise beam time estimate that is independent of the cross section as it is assumed by the Genova-EG event generator.

(k_{10}, Q^2)	$(5.75\,GeV, 3.0 \pm 0.5\,GeV^2)$	$(11\,GeV, 3.0 \pm 0.5\,GeV^2)$	$(11\,GeV, 12.0 \pm 0.5\,GeV^2)$
$N_{ac}^{\pi^+}$	$1.12 \cdot 10^6$	$1.72 \cdot 10^7$	$6.98 \cdot 10^4$
N^{π^+}	$1.41 \cdot 10^5$	$6.26 \cdot 10^6$	$5.18 \cdot 10^4$
$N^{\pi^0 p}$	-	$4.65 \cdot 10^5$	$1.45 \cdot 10^4$
$N^{\eta p}$	-	$1.72 \cdot 10^4$	$1.77 \cdot 10^4$

Table 1: Total number of events N for the $\pi^+(n)$, $\pi^0 p$, and ηp final state and the acceptance corrected one $N_{ac}^{\pi^+}$ for specific kinematic bins focusing on the $S_{11}(1535)$ resonance, with $W = 1535 \pm 100\,MeV$, as an example for the anticipated statistics at an electron beam energy of $k_{10} = 11\,GeV$ gathered in $60\,d$ compared to the measured ones at $k_{10} = 5.75\,GeV$.

Table 1 summarizes the anticipated number of measured events for a specific W and Q^2 bin centered at the $S_{11}(1535)$ resonance. A more general overview is presented in Fig. 32. It shows the generated versus accepted W and Q^2 coverage for both the Genova-EG (middle panels) and the DIS [4] (lower panels) event generator, where the ratio of the accepted over generated events gives the θ and ϕ integrated acceptance. But for any specific W and Q^2 bin we can also generate the corresponding θ and ϕ dependent acceptance functions. Figs. 34-39 present for each final state channel a set of exemplifying plots of the W, Q^2, ϕ, and θ evolutions of the CLAS12 acceptance.

The acceptance and consequently the total number of events, as presented in Table 1, are for the $\pi^0 p$ and ηp final state significantly smaller than for the $\pi^+(n)$ reaction channel. This is due to the fact, that for the neutral meson production channels the single-photon background can only be separated, when both the proton and the neutral meson are detected, which reduces the combined acceptance especially at low momentum transfers, see Figs. 36-39. The missing mass resolution for the neutron in the $\pi^+(n)$ final state is typically better than $40\,MeV$ and increases only for large momentum transfers to a maximum of $80\,MeV$ at $Q^2 = 12\,GeV^2$. The corresponding plots and the neutron missing mass itself are shown in Fig. 40.

---

[3]Taking the different virtual photon fluxes and electron scattering solid angles for both electron beam energies $5.75\,GeV$ and $11\,GeV$ into account.
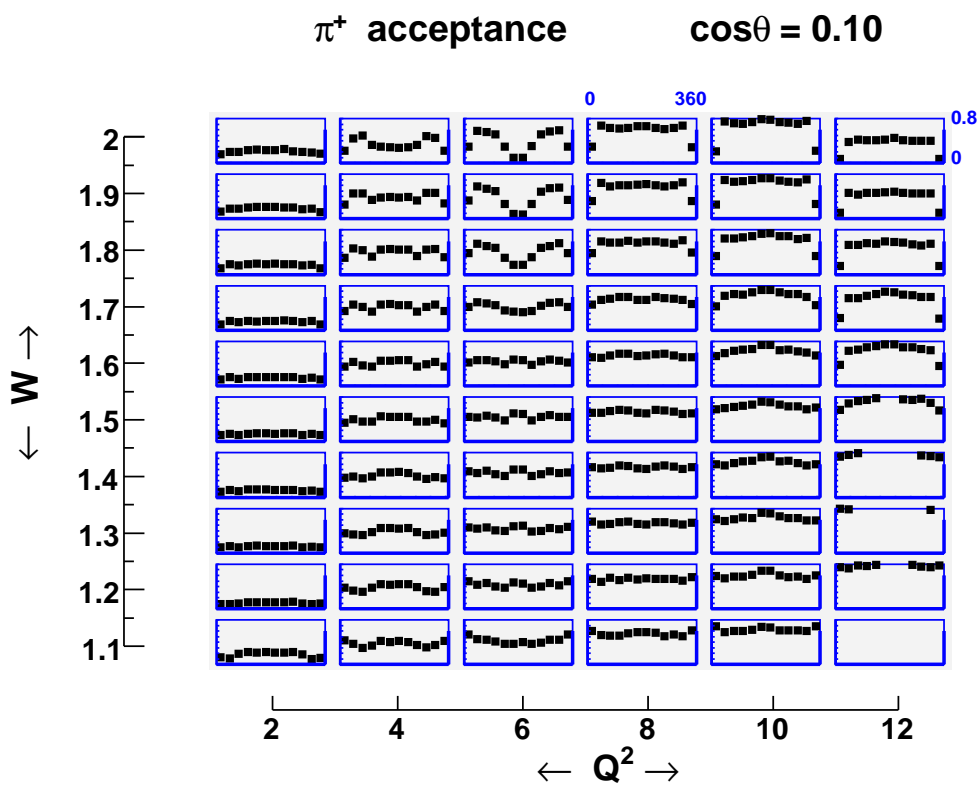
[4]Deep inelastic scattering.

Figure 34: ϕ_π evolution of the π^+ acceptance in the forward $cos\theta_\pi = 0.1 \pm 0.1$ bin for the resonance region and the proposed Q^2 range.

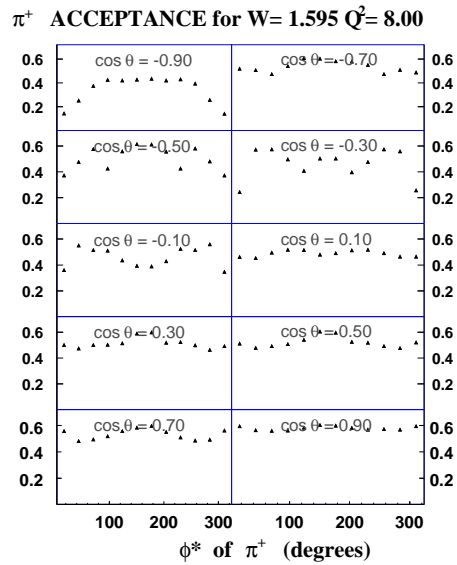Figure 35: ϕ_π evolution of the π^+ acceptance in a specific W and Q^2 bin for the full $cos\theta_\pi$ range.

48

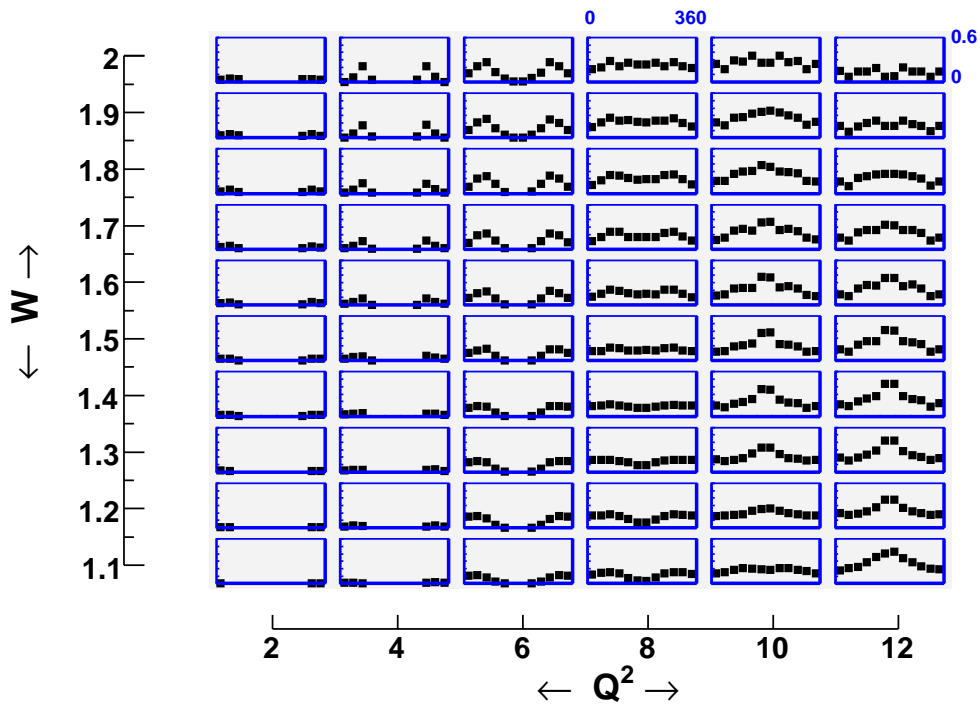Figure 36: ϕ_π evolution of the π^0 acceptance in the forward $cos\theta_\pi = 0.1 \pm 0.1$ bin for the resonance region and the proposed Q^2 range.
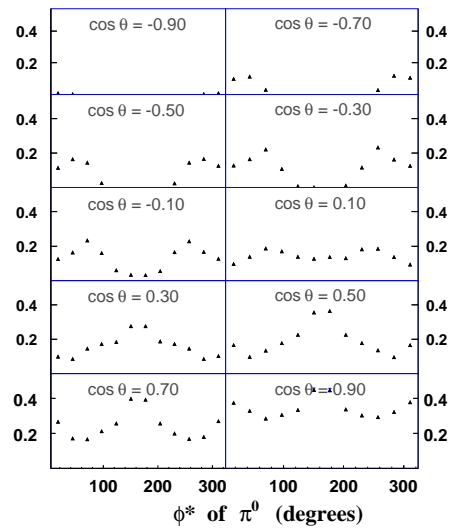

Figure 37: ϕ_π evolution of the π^0 acceptance in a specific W and Q^2 bin for the full $cos\theta_\pi$ range.
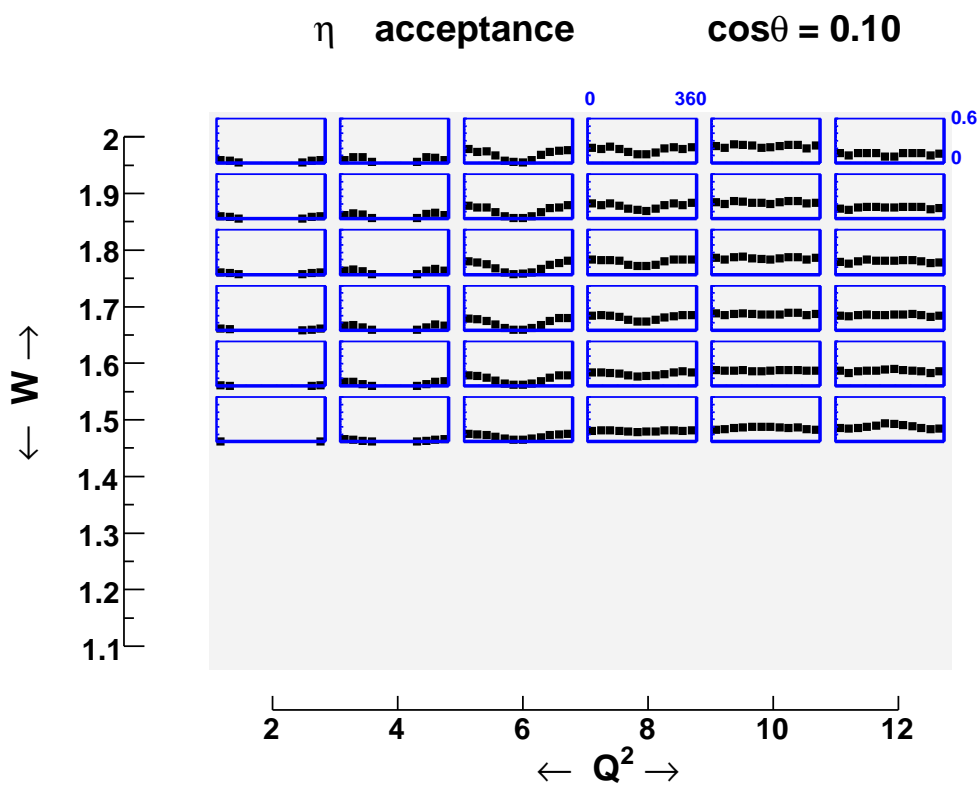
Figure 38: ϕ_η evolution of the η acceptance in the forward $cos\theta_\eta = 0.1 \pm 0.1$ bin for the resonance region and the proposed Q^2 range.

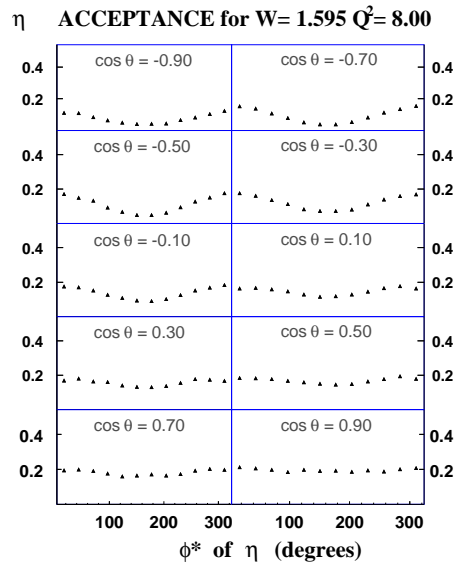Figure 39: ϕ_η evolution of the η acceptance in a specific W and Q^2 bin for the full $cos\theta_\eta$ range.
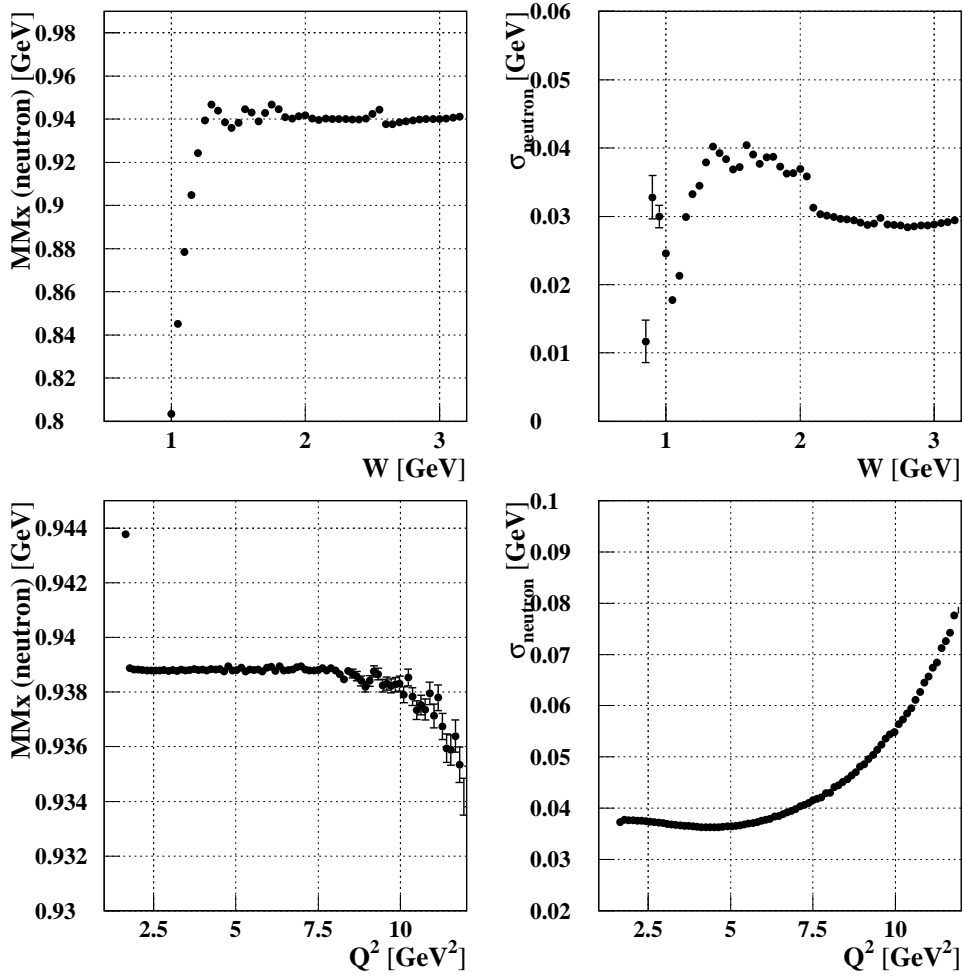
Figure 40: Missing mass (right panels) and missing mass resolution (left panels) for the $\gamma^* p \rightarrow \pi^+(n)$ reaction based on the Genova-EG event generator and the CLAS12 fastmc simulation in dependence of the invariant mass W (upper panels) and the momentum transfer Q^2 (lower panels).

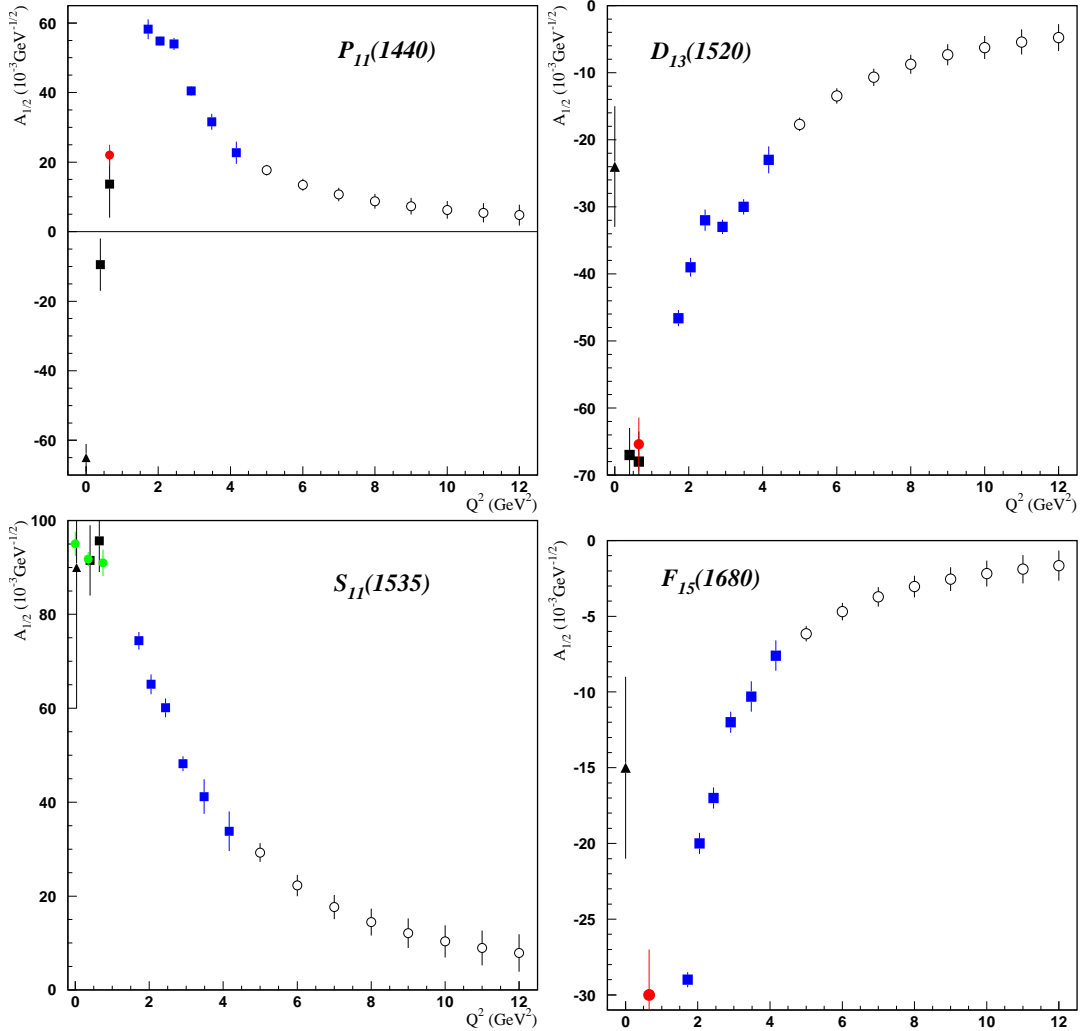# 9 Projected N^* Electro-Coupling, Expected from Proposed Experiments

Figure 41: Projected N^* electro-coupling, expected in proposed experiments (open circles with error bars) . We also present electro-couplings extracted from available CLAS data on 1π electro-production [?] (black filled squares), preliminary data from analysis of e1-6 run (blue filled squares) as well as the results from combined analysis of 1π and 2π electro-production [107].

In this section we demonstrate expected capability of proposed experiment to measure N^* electro-couplings for various states, which were already studied with CLAS at photon virtualities up to 4.5 GeV^2. In Fig. 41 we have presented the projected values of $A_{1/2}$ helicity amplitudes for the electro-excitation of the resonances $P_{11}(1440)$, $D_{13}(1520)$, $S_{11}(1535)$, and $F_{15}(1680)$ at $5 < Q^2 < 12\ GeV^2$. These values are shown along with the existing results

at smaller Q^2. The projected values of helicity amplitudes are obtained via continuation of the results at $Q^2 = 2.91 - 4.16$ GeV^2 according to pQCD behavior $A_{1/2} \sim Q^3$. As it was demonstrated in Fig. 5 such assumption can be applied to the helicity amplitudes of the $P_{11}(1440)$, $D_{13}(1520)$, $S_{11}(1535)$, and $F_{15}(1680)$. The presented errors of projected amplitudes are obtained supposing that the relative errors and amount of data will be close to those obtained in the CLAS experiments for π^+ electro-production at Q^2 from 1.72 to 4.16 GeV^2.

10 Summary and Beam Time Request

In recent years the CLAS Collaboration has succeeded to determine the Q^2 evolution of baryon resonance electro-coupling amplitudes from unpolarized single- and double-pion electro-production data. Consistent results for both channels have been extracted by three different models, the Unitary Isobar Model (UIM) [105, 108], a dispersion theoretical approach [105, 108], and the JLab-MSU isobar model (JM05) [?]. Most of these results are still preliminary, but in the final stage of analysis, which undoubtedly shows that we are able to extract resonance parameters with unprecedented accuracy for many excited states in the mass and four momentum transfer region below $W < 1.7\,GeV$ and $Q^2 < 4.5\,GeV^2$ for single-pion (e1-6 run period) and below $W < 2.0\,GeV$ and $Q^2 < 1.5\,GeV^2$ for double-pion final states (e1 run period).

Within the total requested beam time of $60\,days$ at $11\,GeV$ electron beam energy with the highest possible electron beam polarization, the estimated collected statistics in most of the Q^2 and W bins will be higher and for the highest Q^2 bins comparable to the statistics accumulated in the previous e1 and e1-6 run periods. Furthermore the new results show that the overall resonance to background ratio increases with increasing Q^2. Therefore we are confident that we will be able to extract the resonance electro-coupling amplitudes up to typically $12\,GeV^2$ by using the established model approaches applied to the same number of measured observables, which has been shown to be sufficient for this analysis.

Beam Time Request	Beam	Beam Energy	Luminosity	Target	Detector
$60\,days$	$polarized\ e^-$	$11\,GeV$	$10^{35}\,cm^{-2}s^{-1}$	LH_2	$base\ equipment$

Bibliography

[40] N. Isgur and G. Karl, Phys. Rev. **D19**, 2653 (1979); S. Capstick and N. Isgur, Phys. Rev. D 34, 2809 (1986).

[41] G. Morpurgo, Physics **2**, 95 (1965).

[42] I. C. Cloet, D. B. Leinweber and A. W. Thomas, Phys. Rev. C **65**, 062201 (2002) [arXiv:hep-ph/0203023].

[43] S. Capatick, B. Keister, Phys. Rev. **D51**,3598 (1995).

[44] B. Julia-Diaz, D. O. Riska, and F. Coester, Phys. Rev. **C 69**, 035212 (2004).

[45] M. Aiello, M. M. Giannini, E. Santopinto, J. Phys. G: Nucl. Part. Phys. **24**, 753 (1998); M.De Sanctis, M.M. Giannini, E. Santopinto, A. Vassallo, Phys. Rev. **C76**, 062201 (2007).

[46] I. G. Aznauryan, Phys. Rev. **C78**, 045209 (2008).

[47] C.S. An, Q.B. Li, D.O. Riska, B.S. Zou, Phys.Rev. **C74**, 055205 (2006) ; Erratum-ibid. **C75**, 069901 (2007).

[48] C. D. Roberts, arXiv:0712.0633 [nucl-th] Prog. Part. Nucl. Phys. 61 (2008) pp. 50-65

[49] V.Pascalutsa, M Vanderhaeghen and S. N Yang , Physics Reports **437**,125 (2007)

[50] M. V. Polyakov and K.M.Semenov-Tian-Shansky, arXiv:0811.2901 [hep-ph]

[12] L.L. Frankfurt, M.V. Polyakov, M. Strikman, M. Vanderhaeghen, Phys. Rev. Lett. **84**, 2589 (2000).

[13] K. Goeke, M.V. Polyakov, M. Vanderhaeghen, Prog. Part. Nucl. Phys. **47** 401(2001).

[14] P. Stoler, Phys.Rev.Lett., **91**,172303 (2003).

[51] Alexandrou P. deForcrand, T. Lippert, H. Neff, J. W. Negele, K. Schilling, W. Schroers, and A. Tsapalis, Phys. Rev. D 69, 114506 (2004); C. Alexandrou, P. de Forcrand, H. Neff, J. W. Negele, W. Schroers, and A. Tsapalis, Phys. Rev. Lett. 94, 021601 (2005); C. Alexandrou, T. Leontiou, J.W. Negele, and A. Tsapalis, hep-lat/0608025.

[52] B. Julia-Diaz, T.-S. H. Lee, T. Sato, and C. Smith, Phys. Rev. **C75**, 015205 (2007).

[53] Huey-Wen Lin, Saul D. Cohen, Robert G. Edwards, David G. Richards (Jefferson Lab) . JLAB-THY-08-805, Mar 2008. 4pp. e-Print: arXiv:0803.3020 [hep-lat]

[54] White paper of JLAB Workshop "Electromagnetic $N - N^*$ Transition Form Factors", Newport News, USA, October 13-15, 2008.

[55] V. M. Braun *et al.*, "Electroproduction of the $N^*(1535)$ resonance at large momentum transfer", in progress.

[56] V. M. Braun, A. Lenz, N. Mahnke and E. Stein, Phys. Rev. D **65**, 074011 (2002); V. M. Braun, A. Lenz and M. Wittmann, Phys. Rev. D **73**, 094019 (2006).

[57] A. Matsuyama, T. Sato, and T.-S.H. Lee, Phys. Rep. **439**, 193 (2007).

[58] B. Julia-Diaz, T.-S. H. Lee, and A. Matsuyama, T. Sato, Phys. Rev. (2007)

[59] B. Julia-Diaz, T.-S. H. Lee, A. Matsuyama, T. Sato, and C. Smith, (2008)

[60] T. Sato and T.-S. H. Lee, Phys. Rev. C **54**, 2660 (1996).

[61] S. Kamalov and Shin-Nan Yang, Phys. Rev. Lett, **83**, 4494 (1999)

[149] V. D. Burkert, in "Electromagnetic Interactions and Hadronic Structure", ed by F. Close, S. Donnachie, G. Shaw, Cambridge Monographs on Particle Physics, Nuclear Physics and Cosmology 77 (2007).

[150] V. D. Burkert, Prog. Part Nucl. Phys. **55**, 108 (2005).

[151] V. Burkert and T. S.-H. Lee, Int. J. Mod. Phys. **E13**, 1035 (2004).

[109] I. G. Aznauryan *et al.*, CLAS Collaboration, Phys. Rev. C **78**, 045209 (2008).

[172] V. I. Mokeev *et al.*, Proceedings of the 11th Workshop on the Physics of Excited Nucleons. NSTAR2007, Springer, ed. by H-W. Hammer, V.Kleber, U.Thoma, H. Schmieden, arXiv:0710.5616[hep-ex].

[67] A. Holl *et al.*, Phys. Rev. C **71**, 065204 (2005).

[68] G. Eichman *et al.*, Phys. Rev. C **77**, 042202R (2008).

[69] G. Eichman *et al.*, arXiv:0810:1222[nucl-th].

[70] R. T. Cahill *et al.*, Phys. Rev. D **36**, 2804(1987).

[71] R. T. Cahill *et al.*, Austral. J. Phys. **42**, 2804(1987).

[72] I. Cloet *et al.*, arXiv:0812:0416[nucl-th].

[73] P. O. Bowman *et al.*, Nucl. Phys. Proc. Suppl. **119**, 323(2003).

[74] V. D. Burkert, *et al.*, Phys. Rev. **C67**, 035204 (2003).

[75] M. Burkardt and S. Dalley, Prog. Part. Nucl. Phys. **48**, 317 (2002).

[40] N. Isgur and G. Karl, Phys. Rev. **D19**, 2653 (1979); S. Capstick and N. Isgur, Phys. Rev. D 34, 2809 (1986).

[41] G. Morpurgo, Physics **2**, 95 (1965).

[42] I. C. Cloet, D. B. Leinweber and A. W. Thomas, Phys. Rev. C **65**, 062201 (2002) [arXiv:hep-ph/0203023].

[43] S. Capatick, B. Keister, Phys. Rev. **D51**,3598 (1995).

[44] B. Julia-Diaz, D. O. Riska, and F. Coester, Phys. Rev. **C 69**, 035212 (2004).

[45] M. Aiello, M. M. Giannini, E. Santopinto, J. Phys. G: Nucl. Part. Phys. **24**, 753 (1998); M.De Sanctis, M.M. Giannini, E. Santopinto, A. Vassallo, Phys. Rev. **C76**, 062201 (2007).

[46] I. G. Aznauryan, Phys. Rev. **C78**, 045209 (2008).

[47] C.S. An, Q.B. Li, D.O. Riska, B.S. Zou, Phys.Rev. **C74**, 055205 (2006) ; Erratum-ibid. **C75**, 069901 (2007).

[48] C. D. Roberts, arXiv:0712.0633 [nucl-th] Prog. Part. Nucl. Phys. 61 (2008) pp. 50-65

[49] V.Pascalutsa, M Vanderhaeghen and S. N Yang , Physics Reports **437**,125 (2007)

[50] M. V. Polyakov and K.M.Semenov-Tian-Shansky, arXiv:0811.2901 [hep-ph]

[51] Alexandrou P. deForcrand, T. Lippert, H. Neff, J. W. Negele, K. Schilling, W. Schroers, and A. Tsapalis, Phys. Rev. D 69, 114506 (2004); C. Alexandrou, P. de Forcrand, H. Neff, J. W. Negele, W. Schroers, and A. Tsapalis, Phys. Rev. Lett. 94, 021601 (2005); C. Alexandrou, T. Leontiou, J.W. Negele, and A. Tsapalis, hep-lat/0608025.

[52] B. Julia-Diaz, T.-S. H. Lee, T. Sato, and C. Smith, Phys. Rev. **C75**, 015205 (2007).

[53] Huey-Wen Lin, Saul D. Cohen, Robert G. Edwards, David G. Richards (Jefferson Lab) . JLAB-THY-08-805, Mar 2008. 4pp. e-Print: arXiv:0803.3020 [hep-lat]

[54] White paper of JLAB Workshop "Electromagnetic $N - N^*$ Transition Form Factors", Newport News, USA, October 13-15, 2008.

[55] V. M. Braun *et al.*, "Electroproduction of the $N^*(1535)$ resonance at large momentum transfer", in progress.

[56] V. M. Braun, A. Lenz, N. Mahnke and E. Stein, Phys. Rev. D **65**, 074011 (2002); V. M. Braun, A. Lenz and M. Wittmann, Phys. Rev. D **73**, 094019 (2006).

[57] A. Matsuyama, T. Sato, and T.-S. H. Lee, Phys. Rep. **439**, 193 (2007).

[58] B. Julia-Diaz, T.-S. H. Lee, and A. Matsuyama, T. Sato, Phys. Rev. (2007)

[59] B. Julia-Diaz, T.-S. H. Lee, A. Matsuyama, T. Sato, and C. Smith, (2008)

[60] T. Sato and T.-S. H. Lee, Phys. Rev. C **54**, 2660 (1996).

[61] S. Kamalov and Shin-Nan Yang, Phys. Rev. Lett, **83**, 4494 (1999)

[149] V. D. Burkert, in "Electromagnetic Interactions and Hadronic Structure", ed by F. Close, S. Donnachie, G. Shaw, Cambridge Monographs on Particle Physics, Nuclear Physics and Cosmology 77 (2007).

[150] V. D. Burkert, Prog. Part Nucl. Phys. **55**, 108 (2005).

[151] V. Burkert and T. S.-H. Lee, Int. J. Mod. Phys. **E13**, 1035 (2004).

[109] I. G. Aznauryan *et al.*, CLAS Collaboration, Phys. Rev. C **78**, 045209 (2008).

[172] V. I. Mokeev *et al.*, Proceedings of the 11th Workshop on the Physics of Excited Nucleons. NSTAR2007, Springer, ed. by H-W. Hammer, V.Kleber, U.Thoma, H. Schmieden, arXiv:0710.5616[hep-ex].

[67] A. Holl *et al.*, Phys. Rev. C **71**, 065204 (2005).

[68] G. Eichman *et al.*, Phys. Rev. C **77**, 042202R (2008).

[69] G. Eichman *et al.*, arXiv:0810:1222[nucl-th].

[70] R. T. Cahill *et al.*, Phys. Rev. D **36**, 2804(1987).

[71] R. T. Cahill *et al.*, Austral. J. Phys. **42**, 2804(1987).

[72] I. Cloet *et al.*, arXiv:0812:0416[nucl-th].

[73] P. O. Bowman *et al.*, Nucl. Phys. Proc. Suppl. **119**, 323(2003).

[74] V. D. Burkert, *et al.*, Phys. Rev. **C67**, 035204 (2003).

[75] M. Burkardt and S. Dalley, Prog. Part. Nucl. Phys. **48**, 317 (2002).

[76] K. Joo et al., Phys. Rev. Lett. **88**, 122001 (2002).

[77] M. Ungaro *et al.*, Phys. Rev. Lett. **97**, 112003 (2006).

[78] K. Joo *et al.*, Phys. Rev. **C68**, 032201 (2003).

[79] K. Joo *et al.*, Phys. Rev. **C70**, 042201 (2004).

[80] K. Joo *et al.*, Phys. Rev. **C72**, 058202 (2005).

[81] H. Egiyan *et al.*, Phys. Rev, **C73**, 025204 (2006).

[82] A. Biselli *et al.* ,Phys. Rev. **C68**, 035202 (2003).

[83] A. Biselli *et al.*, arXiv: 0804.3079[nucl-ex].

[84] K. Park *et al.*, Phys. Rev. **C77**, 015208 (2008).

[85] R. Thompson *et al.*, Phys. Rev. Lett. **86**, 1702 (2001).

[86] H. Denizli *et al.*, Phys. Rev. **C76**, 015204 (2007).

[87] P. Ambrozewicz *et al.*, Phys. Rev. **C75**, 045203 (2007).

[88] I. Aznauryan *et al.*, arXiv: 0804.0447[nucl-ex].

[89] D. Carman *et al.*, Phys. Rev. Lett. **90**, 131804 (2003).

[90] R. De Vita *et al.*, Phys. Rev. Lett. **88**, 082001 (2002).

[145] M. Ripani *et al.*, Phys. Rev. Lett. **91**, 022002 (2003).

[147] G. V. Fedotov *et al.*, Bull. of Russian Acad. of Scince **71**, 328 (2007).

[148] G. V. Fedotov *et al.*, (CLAS Collaboration), arXiv:0809.1562 [nucl-ex].

[149] V. D. Burkert, in "Electromagnetic Interactions and Hadronic Structure", ed by F. Close, S. Donnachie, G. Shaw, Cambridge Monographs on Particle Physics, Nuclear Physics and Cosmology 77 (2007).

[150] V. D. Burkert, Prog. Part Nucl. Phys. **55**, 108 (2005).

[151] V. Burkert and T. S.-H. Lee, Int. J. Mod. Phys. **E13**, 1035 (2004).

[97] G. Penner and U. Mosel, Phys. Rev. **C65**, 055202 (2002).

[152] T. P. Vrana, S. A. Dytman and T-S. H. Lee, Phys. Rep. **32B**, 184 (2000).

[99] A. Matsuyama, T. Sato and T.-S. H. Lee, Phys. Rep. **439**, 193 (2007).

[100] T. S.-H. Lee, J. Phys. Conf. Ser. **69**, 012013 (2007).

[101] T. S.-H. Lee and L. C. Smith, J. Phys. **G34**, S83 (2007).

[102] G. F. Chew, M. L. Goldberger, F. E. Low, and Y. Nambu, Phys. Rev. **106**, 1345 (1957).

[103] S. Fubini, Y. Nambu, and V. Watagin, Phys. Rev. **111**, 329 (1958).

[104] D. Drechsel, O. Hanstein, S. Kamalov, and L. Tiator, Nucl. Phys. A **645**, 145 (1999).

[105] I. G. Aznauryan, Phys. Rev. C **67**, 015209 (2003).

[106] R. L. Walker, Phys. Rev. **182**, 1729 (1969).

[107] I. G. Aznauryan, V. D. Burkert, H. Egiyan, *et al.*,Phys. Rev. C **71**, 015201 (2005).

[108] I. G. Aznauryan, V. D. Burkert, *et al.*,Phys. Rev. C **72**, 045201 (2005).

[109] I. G. Aznauryan et al., CLAS Collaboration, Phys. Rev. C **78**, 045209 (2008).

[110] K. Joo et al., CLAS Collaboration, Phys. Rev. Lett. **88**, 122001 (2002).

[111] K. Joo et al., CLAS Collaboration, Phys. Rev. C **68**, 032201 (2003).

[112] K. Joo et al., CLAS Collaboration, Phys. Rev. C **70**, 042201 (2004).

[113] H. Egiyan et al., CLAS Collaboration, Phys. Rev. C **73**, 025204 (2006).

[114] M. Ungaro et al., CLAS Collaboration, Phys. Rev. Lett. **97**, 112003 (2006).

[115] K. Park *et al.*,CLAS Collaboration, Phys. Rev. C **77**, 015208 (2008).

[116] L. Andivanis et al., Phys. Rev. D **4**, 45 (1971).

[117] Ch. Berger et al., Phys. Lett. B **35**, 87 (1971).

[118] W. Bartel et al., Nucl. Phys. B **58**, 429 (1973).

[119] A. F. Still et al., Phys. Rev. D **48**, 29 (1993).

[120] R. C. Walker et al., Phys. Rev. D **49**, 5671 (1994).

[121] L. Andivanis et al., Phys. Rev. D **50**, 5491 (1994).

[122] M. K. Jones et al., Phys. Rev. Lett. **84**, 1398 (2000).

[123] O. Gayou et al., Phys. Rev. C **64**, 038202 (2001).

[124] S. Rock et al., Phys. Rev. Lett. **49**, 1139 (1982).

[125] A. Lung et al., Phys. Rev. Lett. **70**, 718 (1993).

[126] W. K. Brooks *et al.*,Nucl. Phys. A **755**, 261 (2005).

[127] J. Arrington, W. Melnitchouk, J. A. Tjon, Phys. Rev. C **76**, 035205 (2007).

[128] R. Madey *et al.*,Phys. Rev. Lett. **91**, 122002 (2003).

[129] C. J. Bebek *et al.*,Phys. Rev. **D13**, 25 (1976).

[130] C. J. Bebek *et al.*,Phys. Rev. **D17**, 1693 (1978).

[131] T. Horn *et al.*,Phys. Rev. Lett. **97**, 192001 (2006).

[132] V. Tadevosyan *et al.*,Phys. Rev. C **75**, 055205 (2007).

[133] V. Eletski and Ya. Kogan, Yad. Fiz. **39**, 138 (1984).

[134] I. Aznauryan and K. Oganessyan, Phys. Lett. B **249**, 309 (1990).

[156] D. Luke and P. Söding Springer Tracts in Modern Physics 59, (1971).

[165] M. Ripani *et al.*,Nucl. Phys. **A672**, 220 (2000).

[166] V. Mokeev *et al.*,Phys. Atom. Nucl. **64**, 1292 (2001).

[167] V. Mokeev *et al.*,Phys. Atom. Nucl. **66**, 1322 (2003).

[168] I. G. Aznauryan *et al.*, Phys. Rev. **C72**, 045201 (2005).

[169] V. I. Mokeev, V. D. Burkert, *et al.*,Proc. of the Workshop on the Physics of Excited Nucleon. NSTAR2005, ed. by S.Capstick, V.Crede, P.Eugenio,hep-ph/0512164.

[170] V. D. Burkert, *et al.*,Phys. Atom. Nucl. **70**, 427 (2007).

[171] V. I. Mokeev and V. D. Burkert, J. Phys. Conf. Ser **69**, 012019 (2007),hep-ph/0701056.

[172] V. I. Mokeev *et al.*,Proceedings of the 11th Workshop on the Physics of Excited Nucleons. NSTAR2007, Springer, ed. by H-W. Hammer, V.Kleber, U.Thoma, H. Schmieden, arXiv:0710.5616[hep-ex]

[173] V. I. Mokeev *et al.*,arXiv: 0809.4158[hep-ph].

[145] M. Ripani *et al.*, Phys. Rev. Lett. **91**, 022002 (2003).

[146] E. Isupov, private communication

[147] G. V. Fedotov *et al.*, Bull. of Russian Acad. of Scince **71**, 328 (2007).

[148] G. V. Fedotov *et al.*,(CLAS Collaboration), arXiv:0809.1562 [nucl-ex], accepted by PRC.

[149] V. D. Burkert, in "Electromagnetic Interactions and Hadronic Structure", ed by F. Close, S. Donnachie, G. Shaw, Cambridge Monographs on Particle Physics, Nuclear Physics and Cosmology 77 (2007).

[150] V. D. Burkert, Prog. Part Nucl. Phys. **55**, 108 (2005).

[151] V. Burkert and T. S.-H. Lee, Int. J. Mod. Phys. **E13**, 1035 (2004).

[152] T. P. Vrana, S. A. Dytman and T-S. H. Lee, Phys. Rep. **32B**, 184 (2000).

[156] D. Luke and P. Söding Springer Tracts in Modern Physics 59, (1971).

[154] U. Thoma, Int. J. Mod. Phys. **A20**, 280 (2005).

[155] A. Anisovich, E. Klempt, A. Sarantsev and U. Thoma, Eur. Phys. J.**A24**, 111 (2005).

[156] D. Luke and P. Söding Springer Tracts in Modern Physics 59, (1971).

[157] J. A. Gomez Tejedor and E. Oset, Nucl. Phys. **A600**, 413 (1996).

[158] J. C. Nacher *et al.*,Nucl. Phys. **A674**, 205 (2000).

[159] L. Y. Murphy and J.-M. Laget, DAPNIA-SPHN-96-10.

[160] W. Roberts and A. Rakotovao, JLAB-TH-97-01.

[161] W. Roberts and T. Oed, Phys. Rev. **C71**, 055201 (2005).

[162] M. Hirata, N. Katagiri and T. Takaki, Phys. Rev. **C67**, 034601 (2003).

[163] A. Fix and H. Arenhovel, Eur. Phys. J. **A25**, 115 (2005).

[164] A. Kiswandhi *et al.*,J. Phys. Conf. Ser. **69**, 012018 (2007).

[165] M. Ripani *et al.*,Nucl. Phys. **A672**, 220 (2000).

[166] V. Mokeev *et al.*,Phys. Atom. Nucl. **64**, 1292 (2001).

[167] V. Mokeev *et al.*,Phys. Atom. Nucl. **66**, 1322 (2003).

[168] I. G. Aznauryan *et al.*, Phys. Rev. **C72**, 045201 (2005).

[169] V. I. Mokeev, V. D. Burkert, *et al.*,Proc. of the Workshop on the Physics of Excited Nucleon. NSTAR2005, ed. by S.Capstick, V.Crede, P.Eugenio,hep-ph/0512164.

[170] V. D. Burkert, *et al.*,Phys. Atom. Nucl. **70**, 427 (2007).

[171] V. I. Mokeev and V. D. Burkert, J. Phys. Conf. Ser **69**, 012019 (2007),hep-ph/0701056.

[172] V. I. Mokeev *et al.*,Proceedings of the 11th Workshop on the Physics of Excited Nucleons. NSTAR2007, Springer, ed. by H-W. Hammer, V.Kleber, U.Thoma, H. Schmieden, arXiv:0710.5616[hep-ex]

[173] V. I. Mokeev *et al.*,arXiv: 0809.4158[hep-ph].

[174] M.Bellis, et.al. (CLAS Collaboration), Proceedings of NSTAR2004 workshop , March 24-27, 2004, Grenoble, France, World Scientific, ed. by J.-P. Bocquet, V. Kuznetsov, D. Rebreyend, 139.

[175] M. Battaglieri, et. al. Phys. Rev. Lett. **87**, 172002 (2001).

[176] S. Strauch, *et al.*,Phys. Rev. Lett., accepted, hep-ex/0508002.

[177] U. Thoma, Int. J. Mod. Phys. **A20**, 280 (2005).

[178] C. Wu, et. al. Eur. Phys. J **A23**, 317 (2005).

[179] Y. Assafiri, *et al.*, Phys. Rev. Lett. **90**, 222001 (2003).

[180] J. Ahrens, *et al.*, Phys. Lett. **B624**, 173 (2005).

[181] J. Ahrens, *et al.*, Phys. Lett. **B551**, 49 (2003).

[182] M. Kotulla, *et al.*, Phys. Lett. **B578**, 63 (2004).

[183] W. Langgartner, *et al.*, Phys. Rev. Lett. **87**, 052001-1 (2001).

[184] F. Harter, *et al.*, Phys. Lett. **B401**, 229 (1997).

[185] A. Braghieri, *et al.*, Phys. Lett. **B363**, 46 (1995).

[186] Cambridge Bubble Chamber Group, Phys. Rev. 155, 1477(1967); ABBHHM Collaboration, Phys. Rev. 175, 1669 (1968).

[187] M. Ripani and E.N. Golovach based on P. Corvisiero *et al.*, NIM A **346**, (1994) 433.

[188] CLAS12 Fast MC

[189] L. W. Witlow, *et al.*, Phys. Lett. **B282** 475 (1992).